DE LA RECHERCHE À L'INDUSTRIE
cea

PULSE school 2015

INSTITUT NANOSCIENCES
ET CRYOGÉNIE

A glimpse of
X-Ray diffraction and unique objects

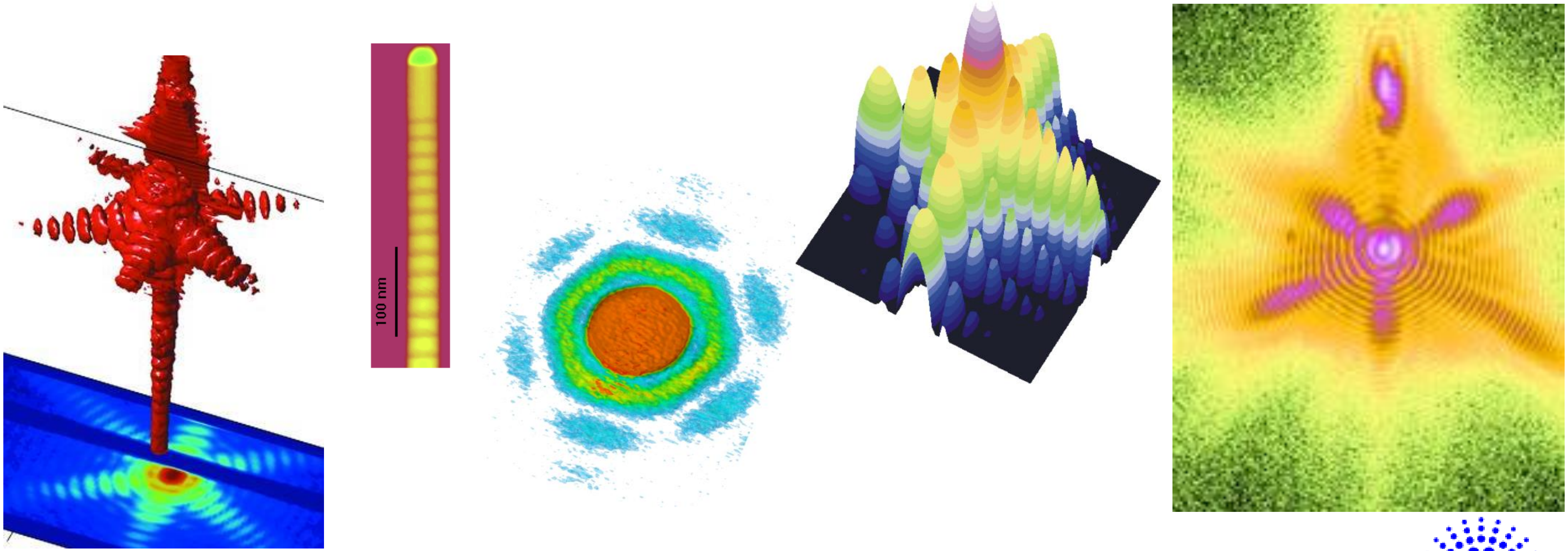

G. Renaud
CEA-Grenoble – INAC , France &
BM32 beamline @ ESRF

gilles.renaud@cea.fr

ESRF

Outline

- **Why X-ray Diffraction on unique objects?**
- **Which X-ray sources? Which focusing devices? Which techniques?**

- **X-ray Scanning Microscopies:**

Composition -Fluorescence Maps (2D) Nanotomography (3D)

Structure -Scanning X-ray Diffraction Microscopy

-Scanning Laue micro-Diffraction

- **Full reconstruction of a single nano-object with coherent x-rays**

-Coherent X-Ray Diffraction

-X-ray Holography

-Bragg Ptychography

- **Conclusions and future directions**

Structural characterization of nanostructures

New physical properties of nanostructures

e.g. Electronic applications

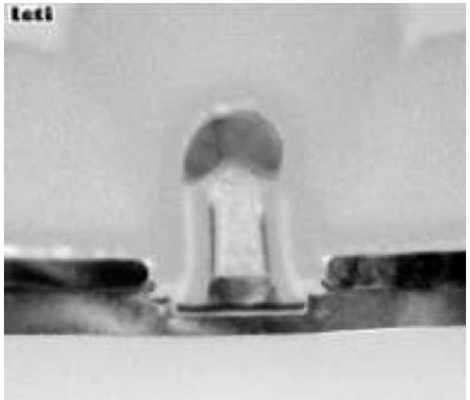

Strain & defects affects/tunes the carrier mobility

e.g. Photonic applications

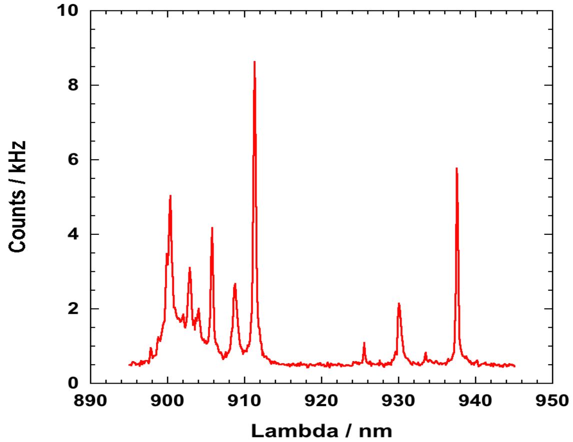

Size and strain & defects affect photoemission

Strongly correlated to structural properties:

- ***atomic structure*** ***(strain, relaxation, defects ...)***
- ***morphology*** ***(shape, size, lateral arrangement …)***
- ***composition*** ***(intermixing, atomic ordering)***

Need accurate size & strain determination → X-ray diffraction

The usual techniques to study nanostructures: Grazing Incidence X-ray Scattering (GIXS / GIXD / GID)

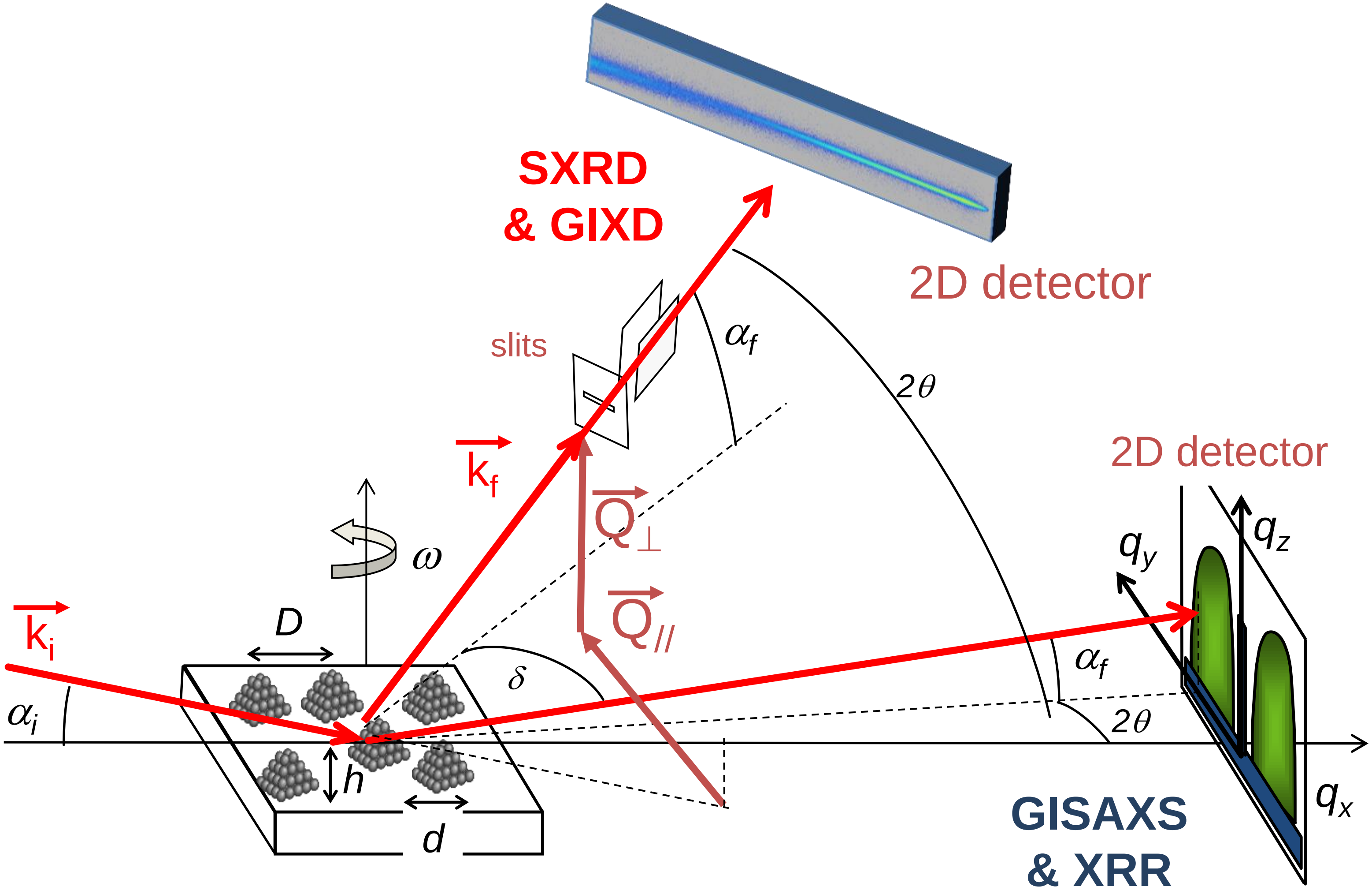

Exploration of reciprocal space with $\mathbf{Q} = \mathbf{k}_f - \mathbf{k}_i$

$\mathbf{Q} = \mathbf{Q}_{//} + \mathbf{Q}_\perp$

Reciprocal space of nanostructure on surface. Ex: Ge/Si(001)

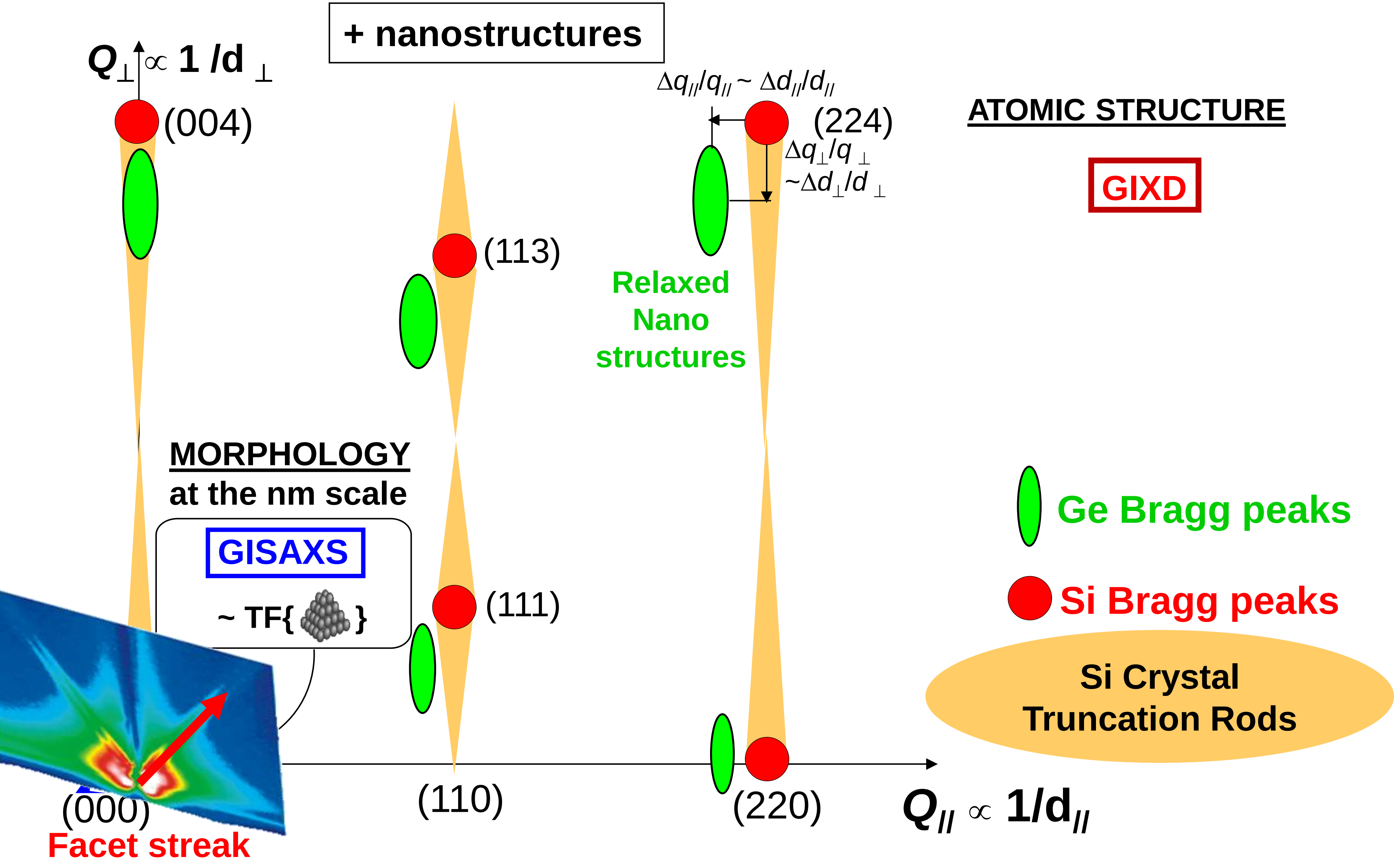

+ nanostructures

ATOMIC STRUCTURE

GIXD

Relaxed Nano structures

MORPHOLOGY at the nm scale

GISAXS

~ TF{ }

Facet streak

Ge Bragg peaks

Si Bragg peaks

Si Crystal Truncation Rods

X-ray studies of individual nanostructures

“standard” experiment

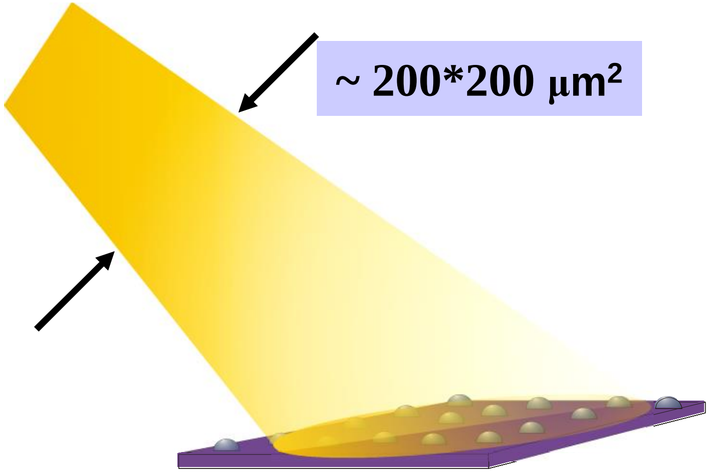

10^4-10^5 objects usually polydisperse
➔ Statistically averaged properties!!!

“nano-beam” experiment

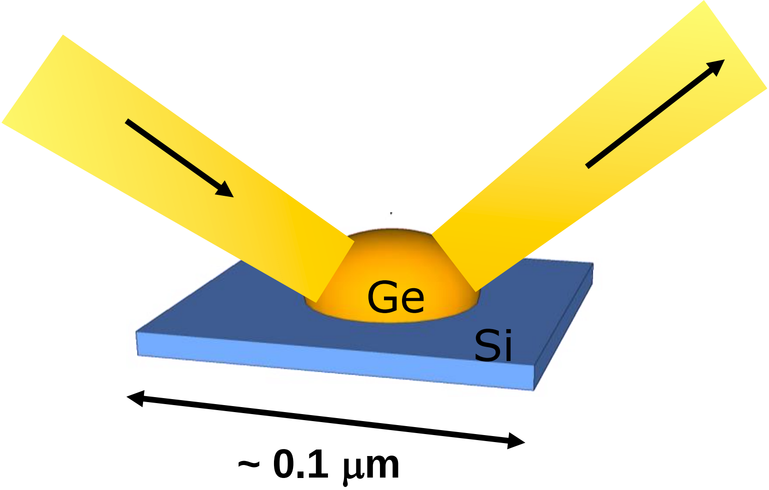

Measurement of individual objects

Need to compensate for less scattering objects ➔

Synchrotron X-ray sources + focusing of the x-ray beam

X-ray sources & nano-focusing of (coherent) X-ray beams

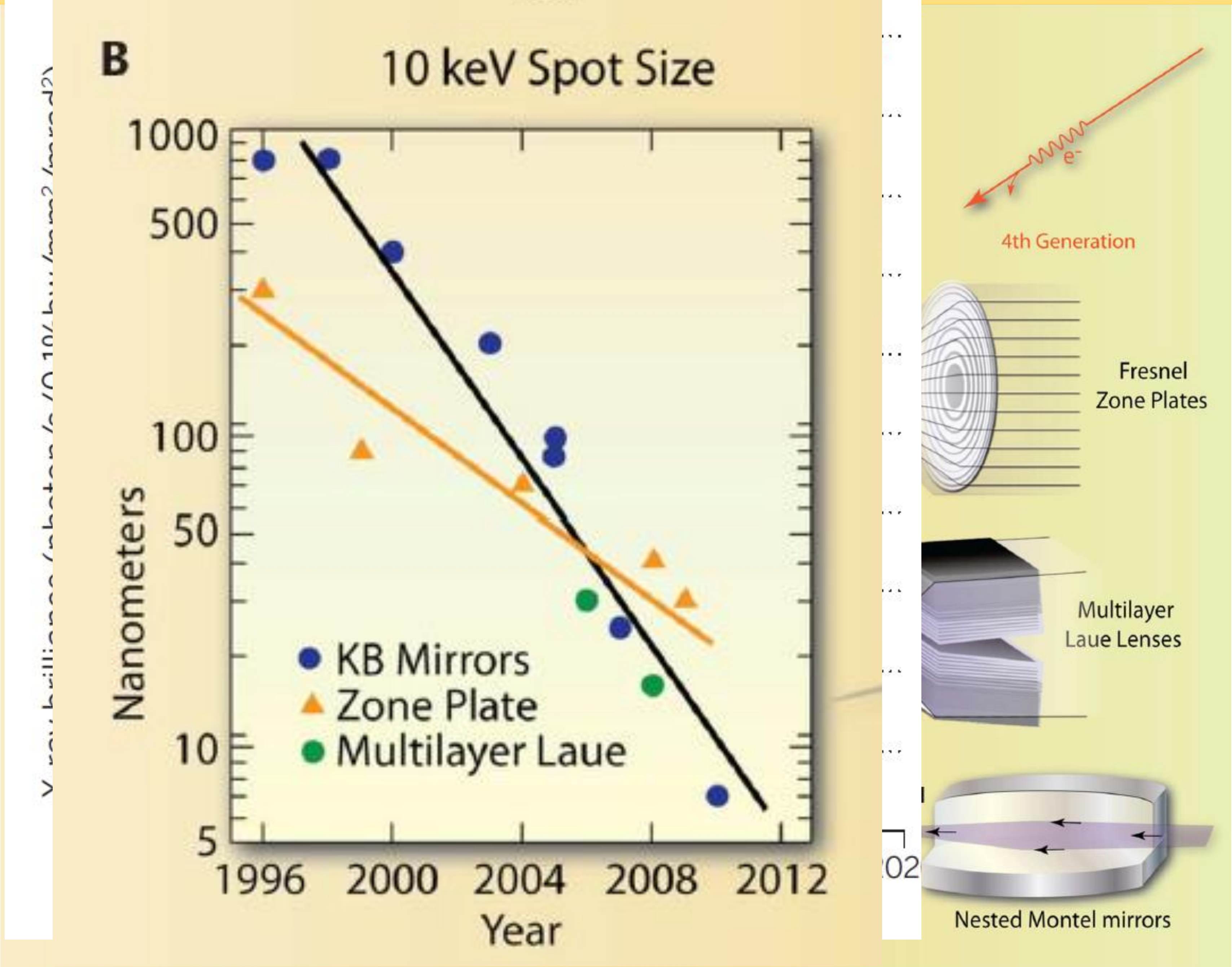

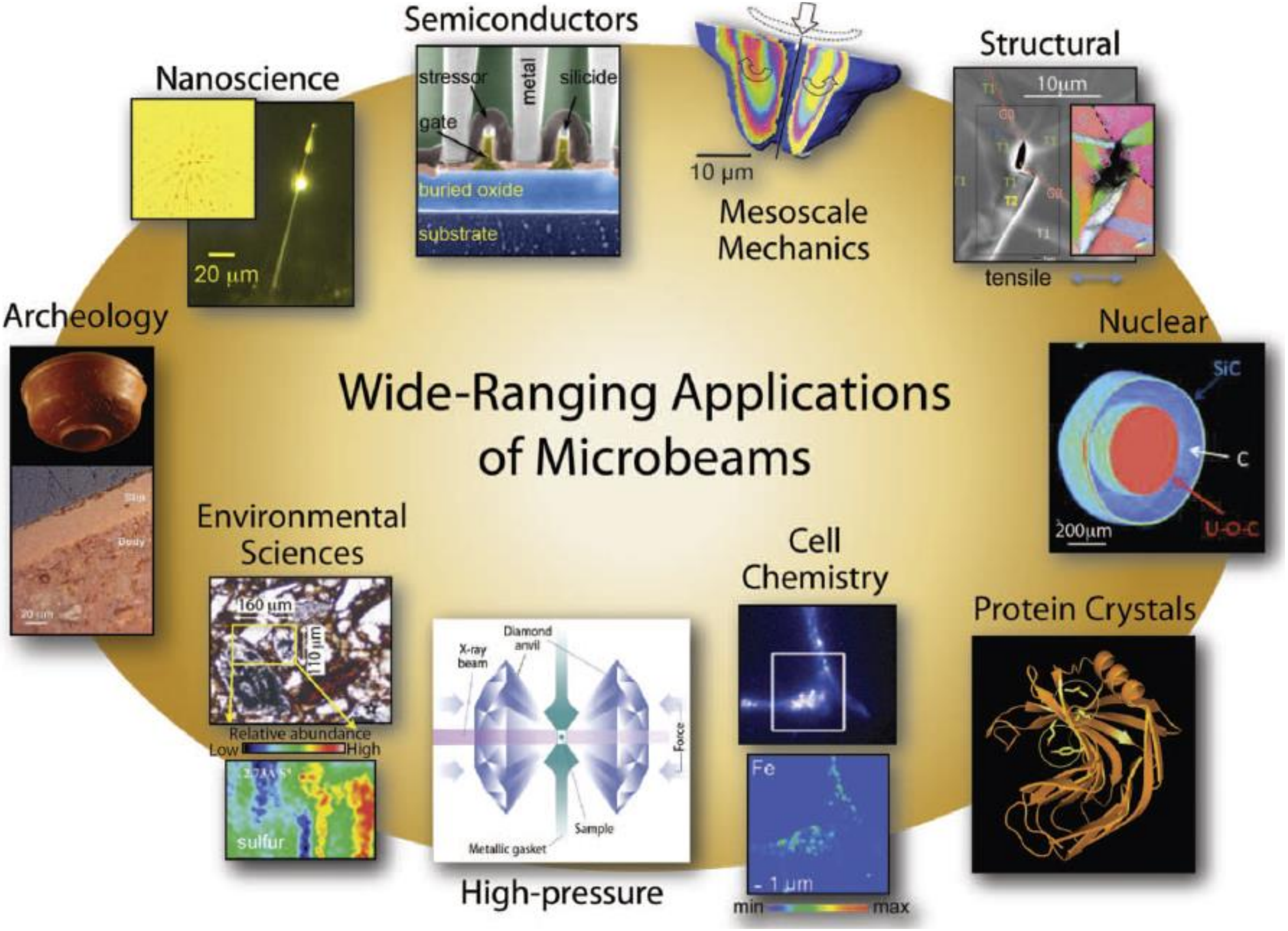
Wide-Ranging Applications of Microbeams
Semiconductors
stressor
metal
silicide
gate
buried oxide
substrate
Nanoscience
20 µm
10 µm
Mesoscale Mechanics
Structural
10µm
T1
G0
T2
tensile
Archeology
Slip
Body
20 µm
Nuclear
SiC
C
U-O-C
200µm
Environmental Sciences
160 µm
110 µm
Relative abundance
Low
High
sulfur
X-ray beam
Diamond anvil
Force
Sample
Metallic gasket
High-pressure
Cell Chemistry
Fe
1 µm
min
max
Protein Crystals

Wide range of techniques → different information

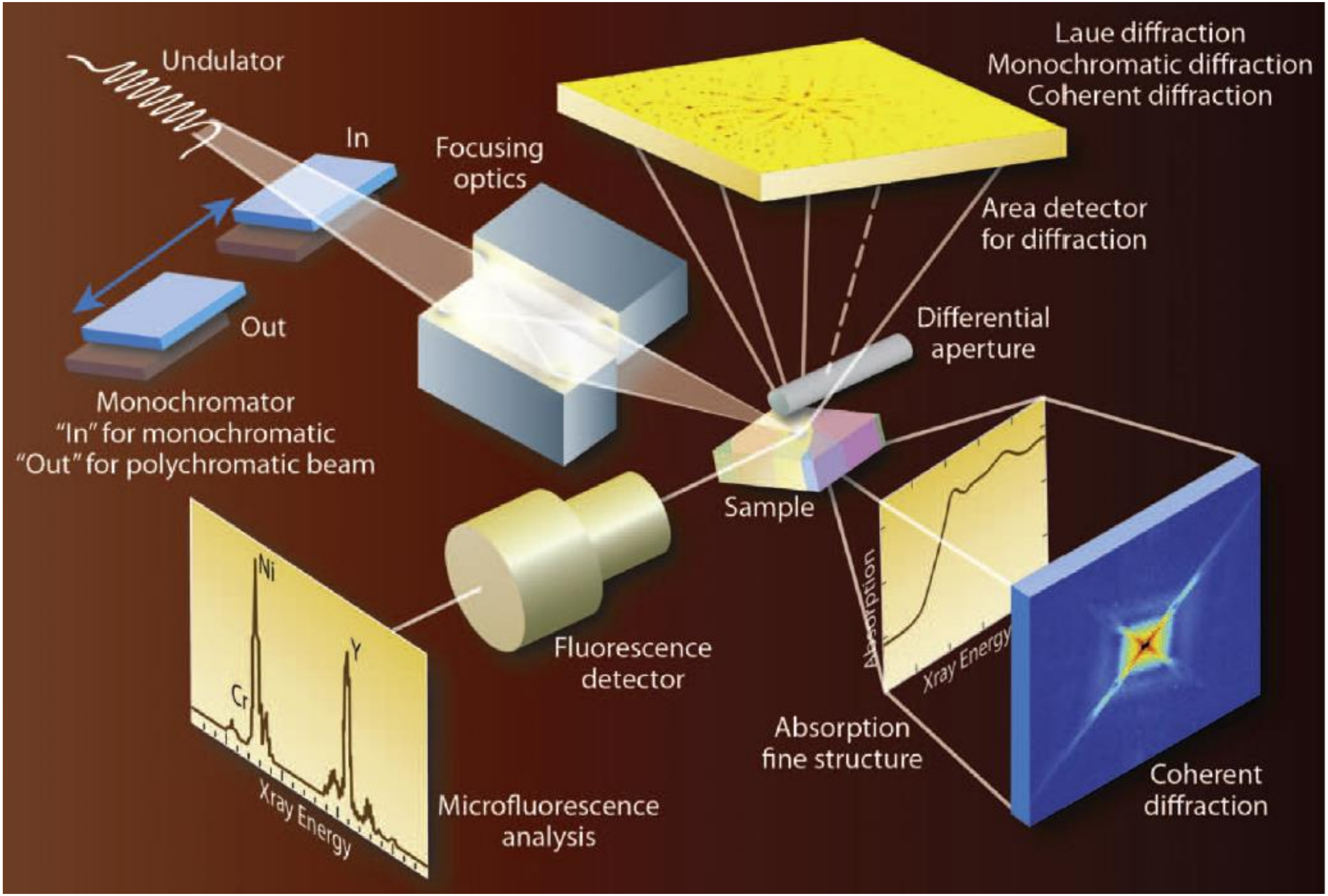

1) Scanning X-ray fluorescence microscopy:

“Seeing” with Fluorescence

Elemental composition maps
Resolution = beamsize, 60 nm ID22 undulator- ESRF Grenoble

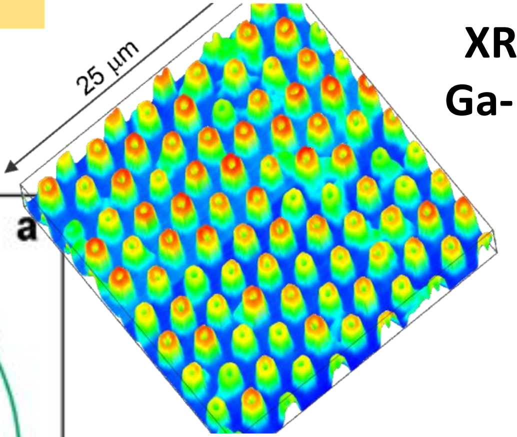

XRF
Ga-K$_\alpha$

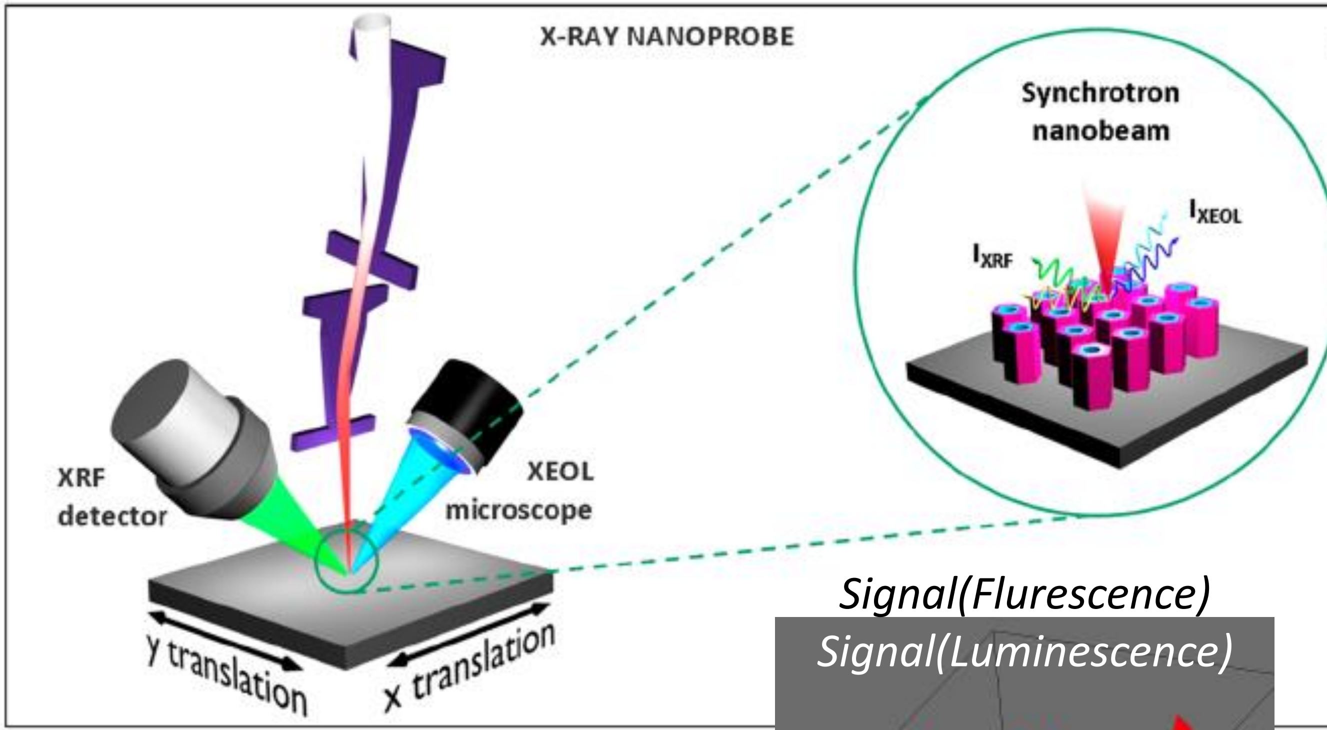

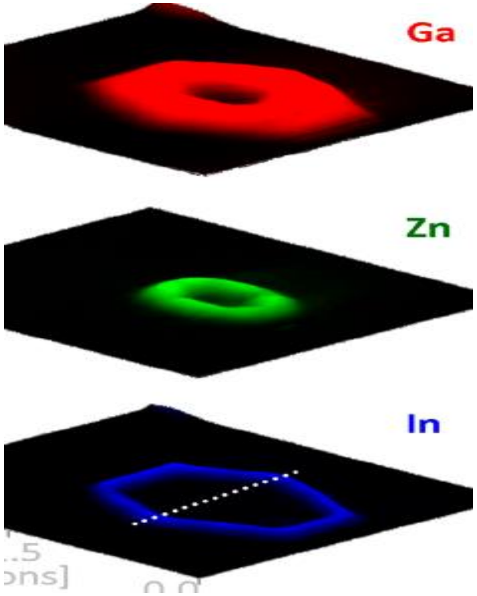

Signal(Flurescence)

Signal(Luminescence)

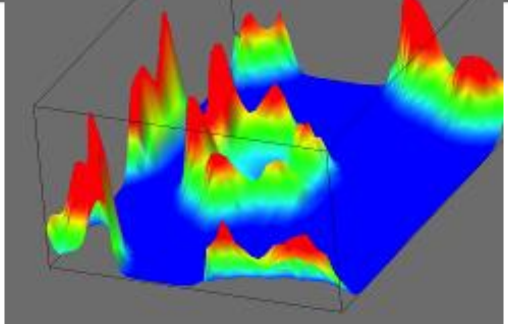

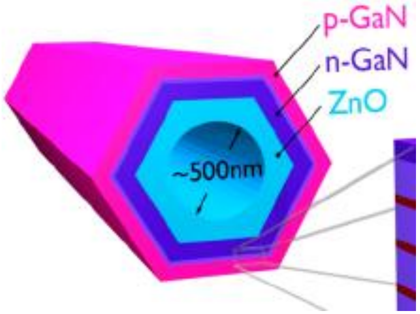

G. Martinez-Criado *et al Nano Lett.* 2012 **12**, 5829−5834

2) Scanning X-ray Diffraction Microscopy:

SXDM - Scanning X-ray Diffraction Microscopy

A tool to investigate the internal structure of devices non-destructively

Sample after TEM

Sample after XRD

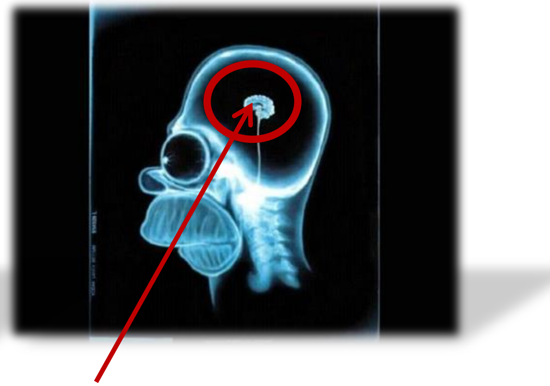

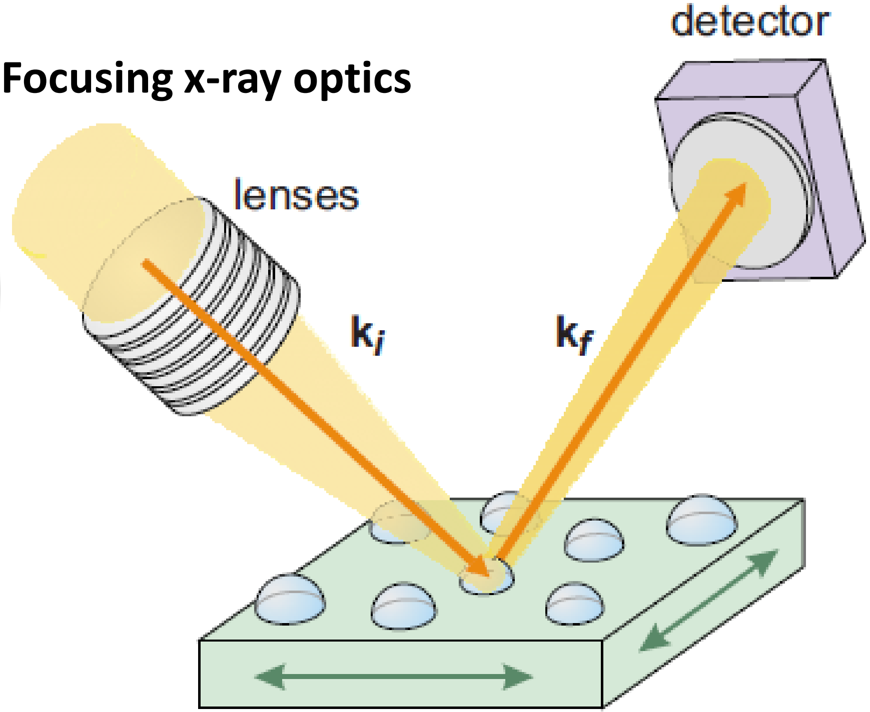

Focusing x-ray optics

- **localize** and study the diffraction signal (lattice parameter - form factor) of **one nanostructure within a device** and correlate it with its environment (e.g. strain).

Mocuta et al. PRB 77, 245425 (2008)

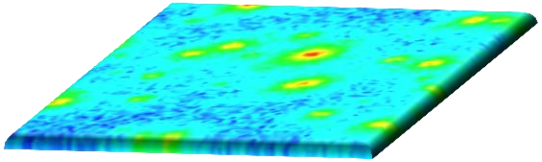

- **Real-space map of the sample at a specific crystallographic orientation.**

Example: SiGe pyramids / Si(001)

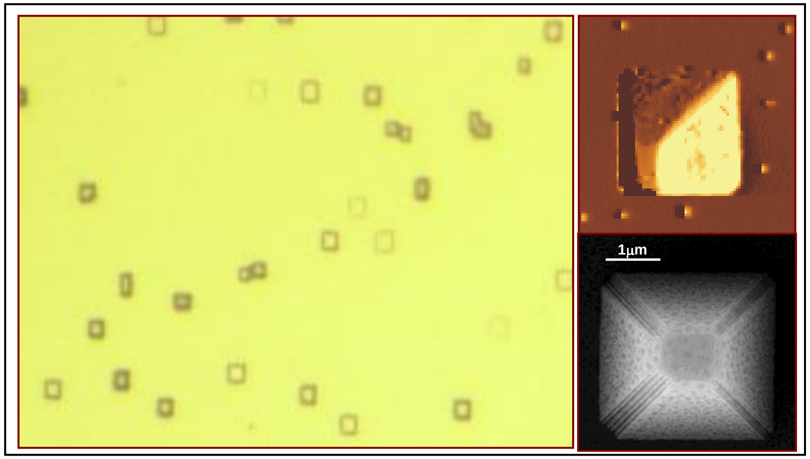

Sample made by LPE
M.Schmidbauer

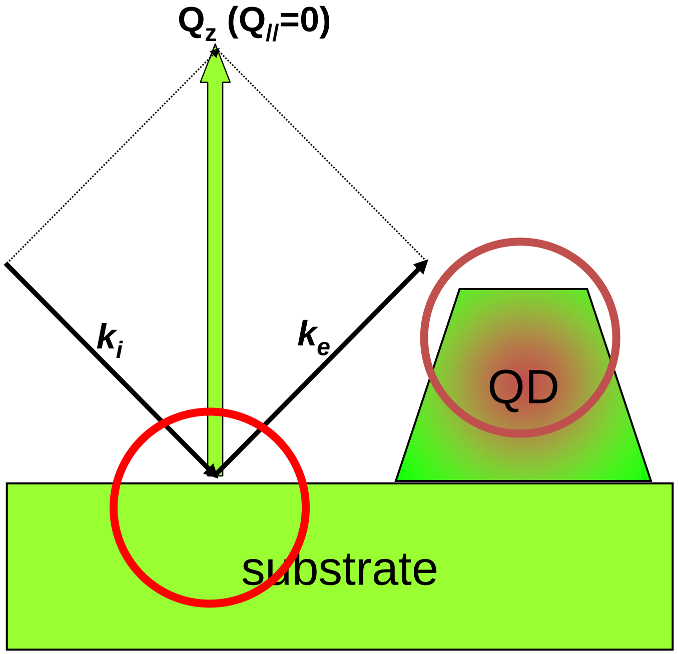

What do we expect to measure ?

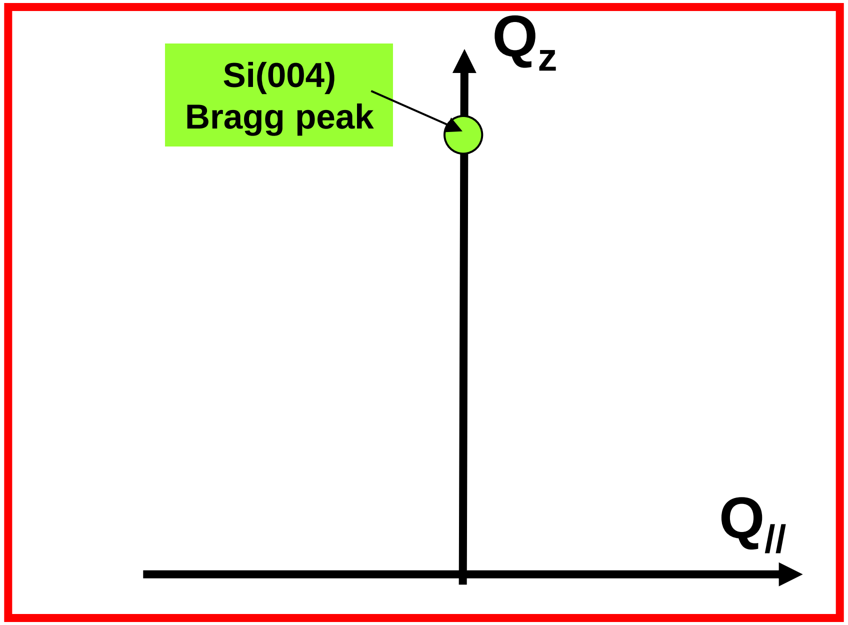

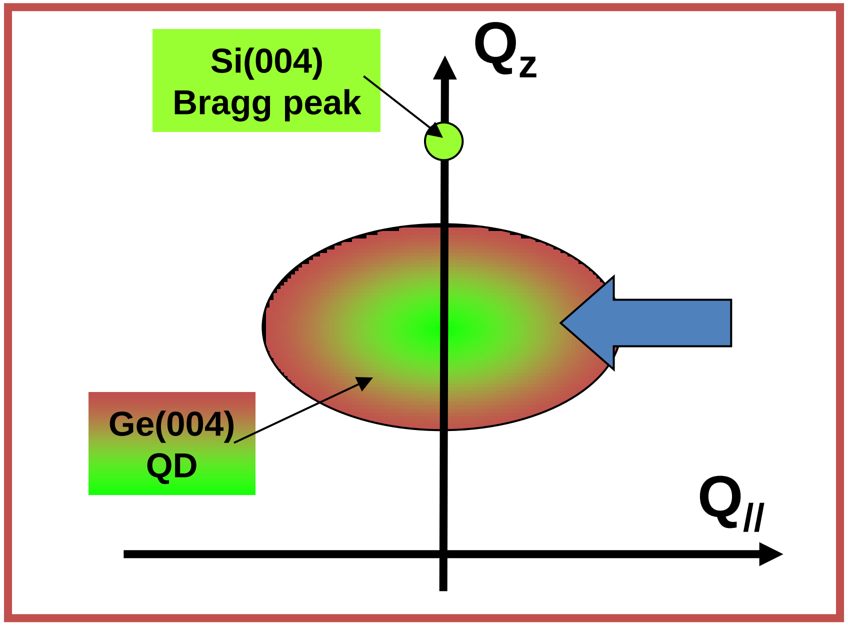

SiGe pyramids - (SDXM)

optical microscope image

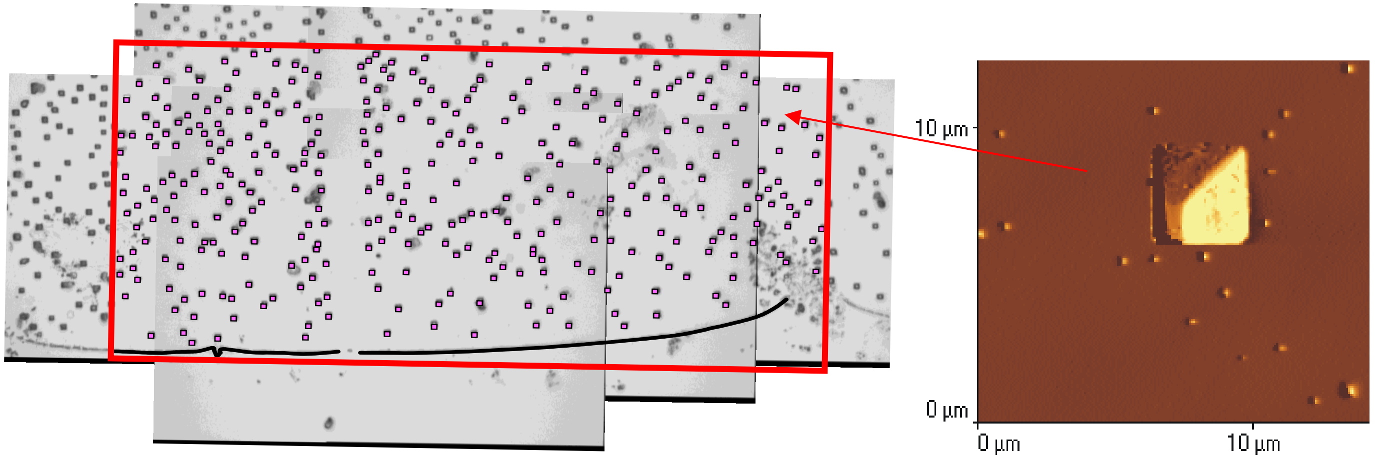

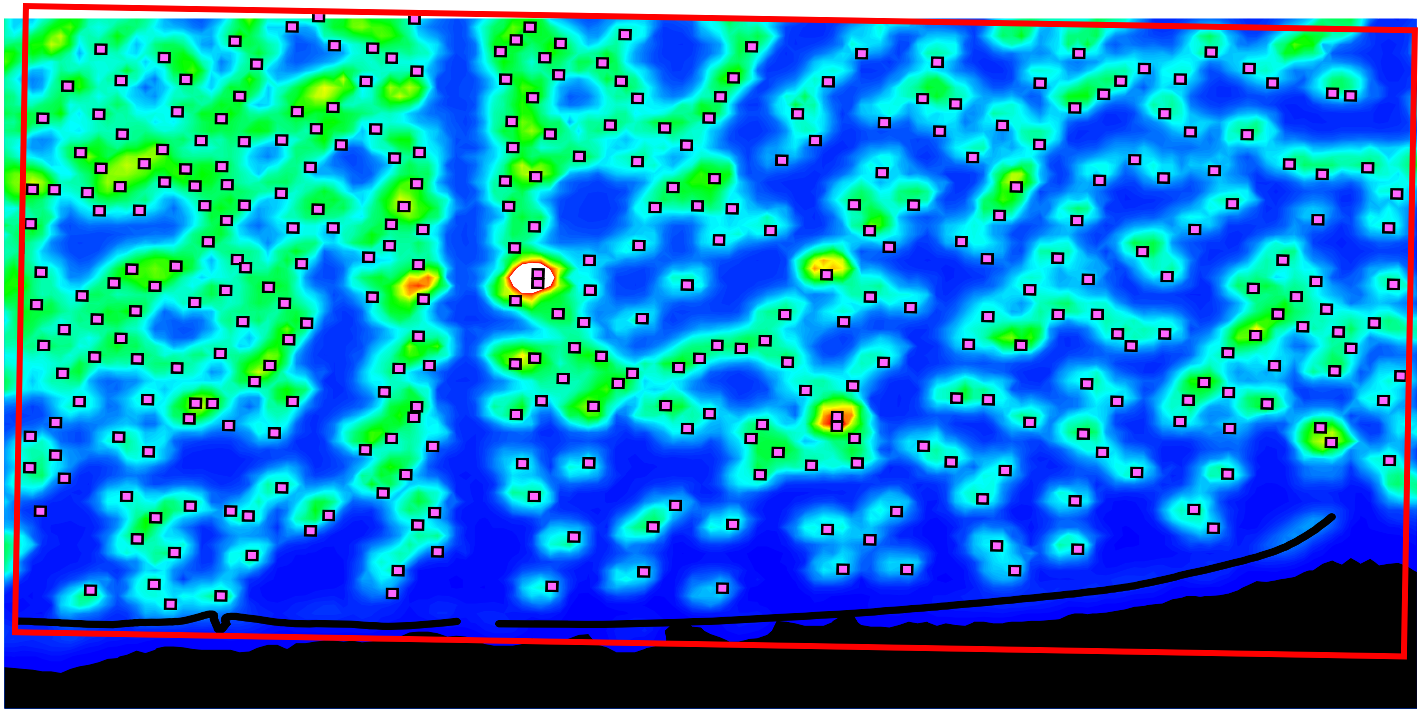

Reciprocal space maps (004)

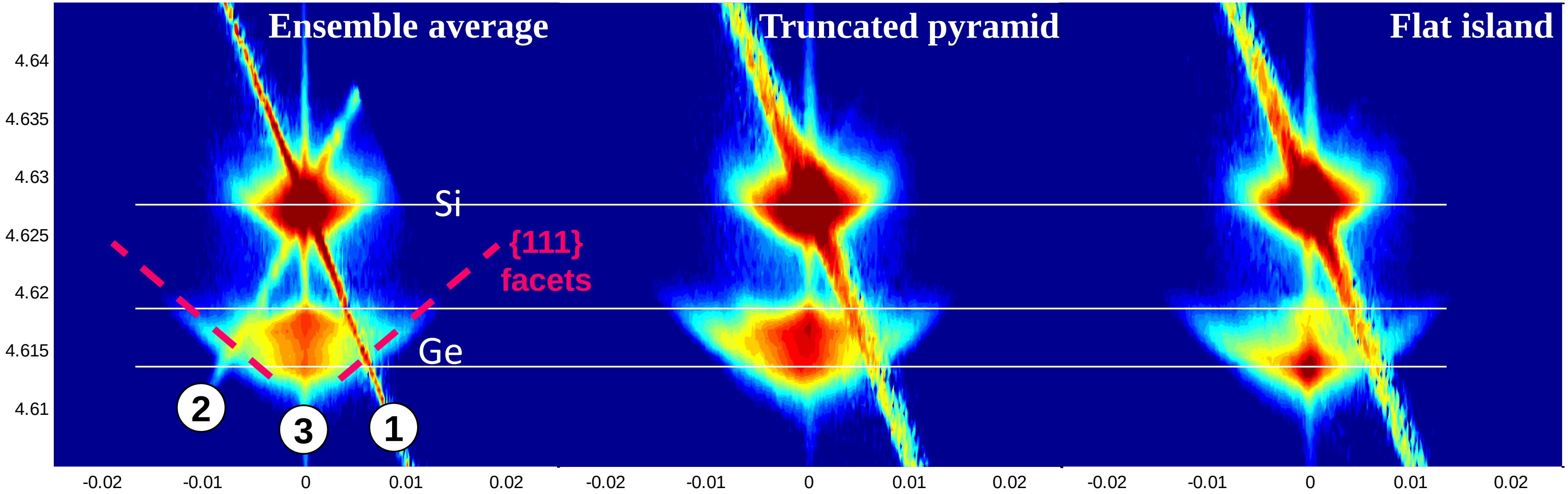

1. **detector streak**
2. **Monochromator streak**
3. **CTR**

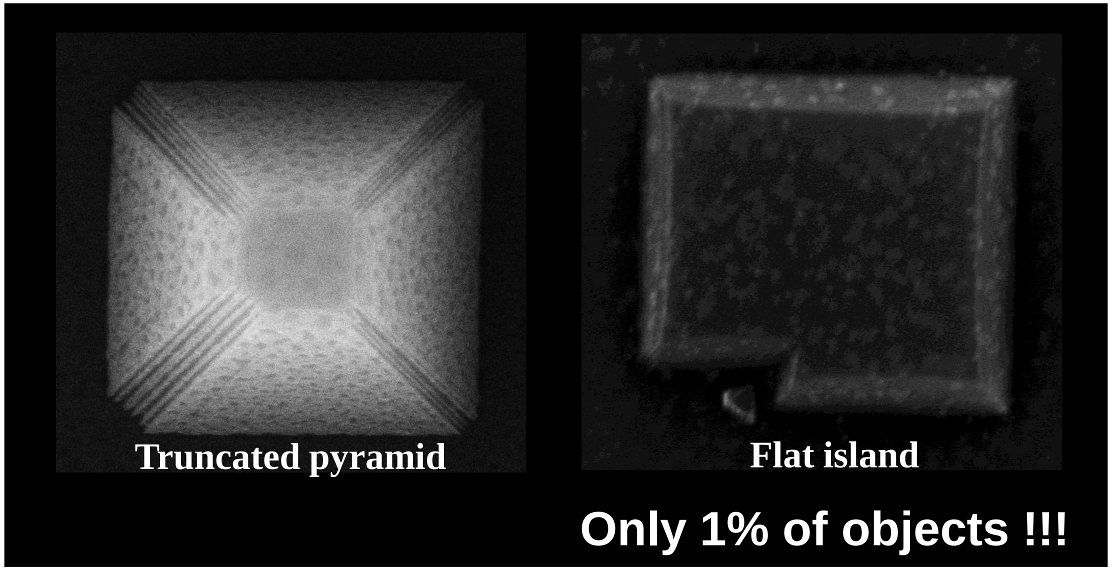

Only 1% of objects !!!

Truncated pyramids (3×3×1.5 μm^3)
~5-10% Ge content
Concentration gradient from base to top

Reciprocal space maps @ (115) Bragg asymmetric reflection

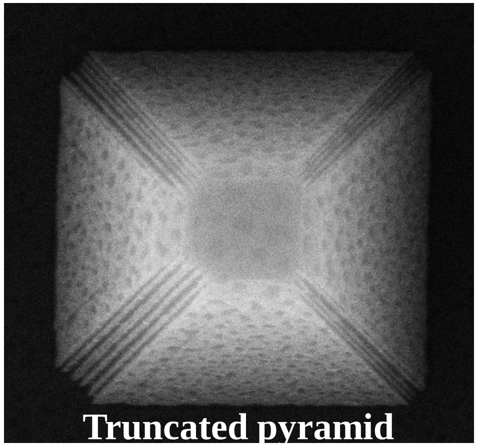

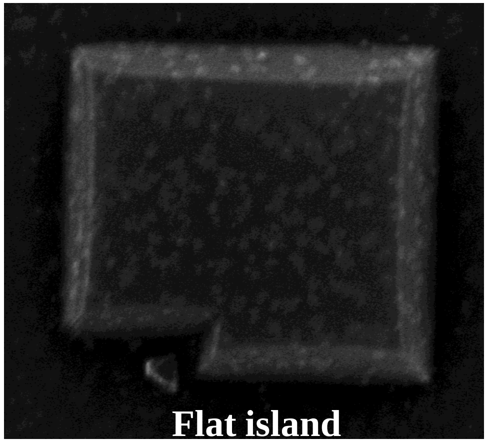

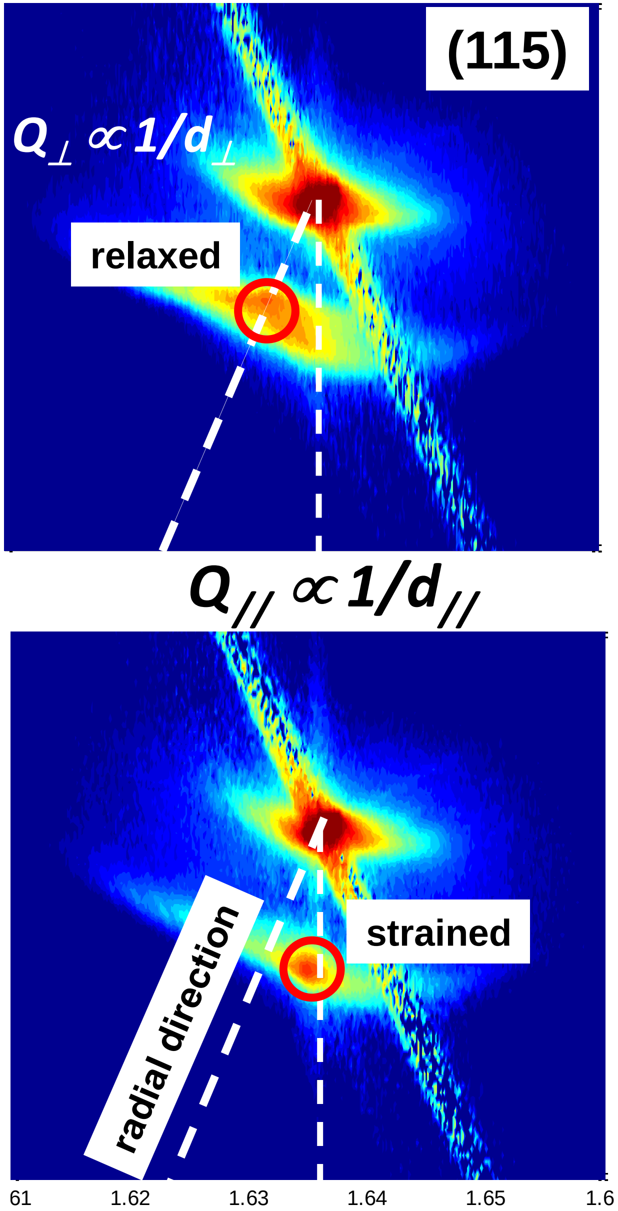

Mocuta et al. PRB 77, 245425 (2008)

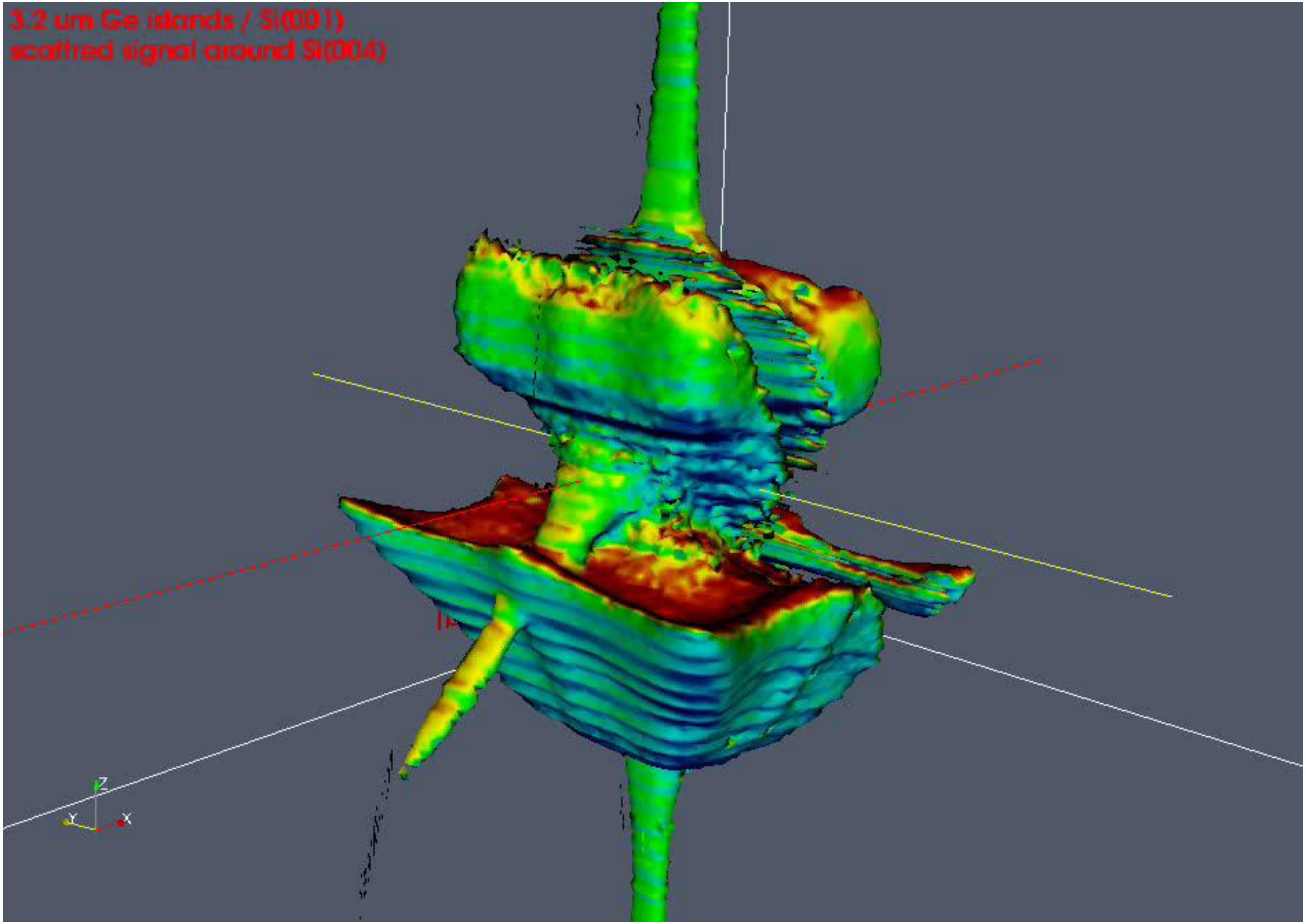
3.2 um Ge islands / Si(001)
scattred signal around Si(004)
Z
Y
X

Tomography of a Bragg peak – data *vs.* simulation

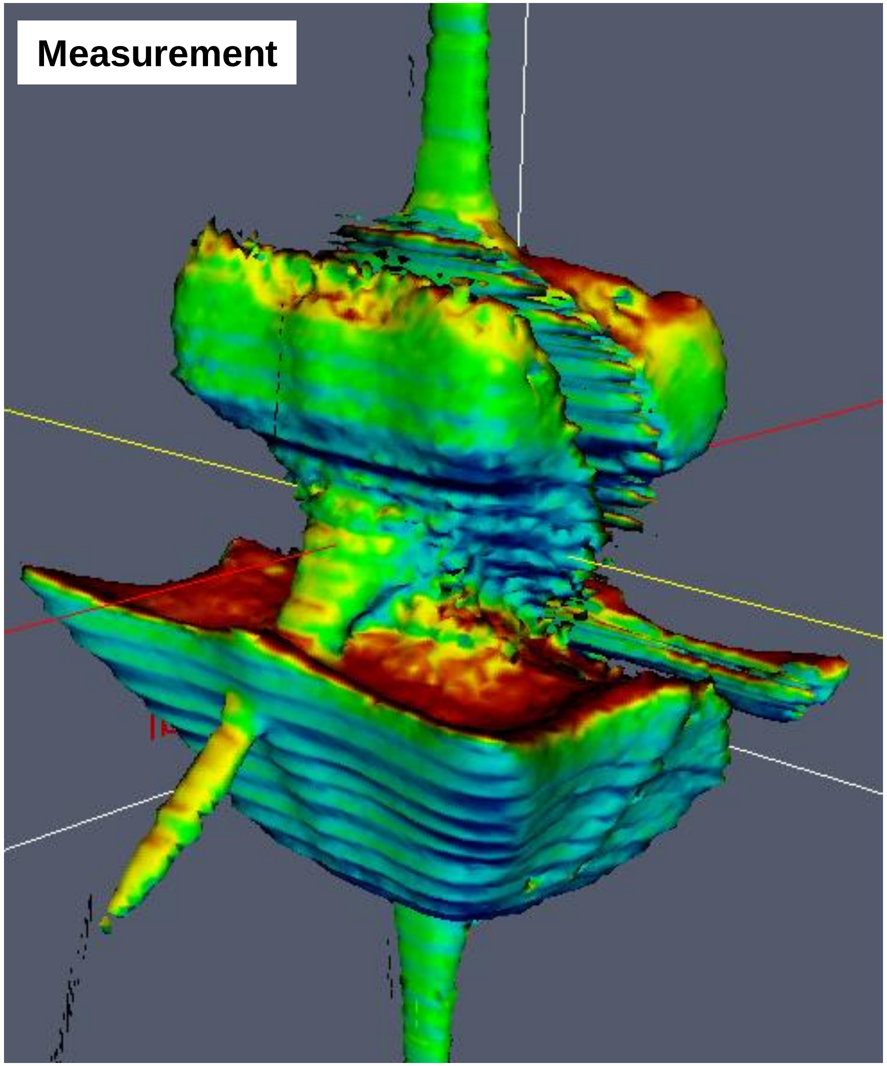

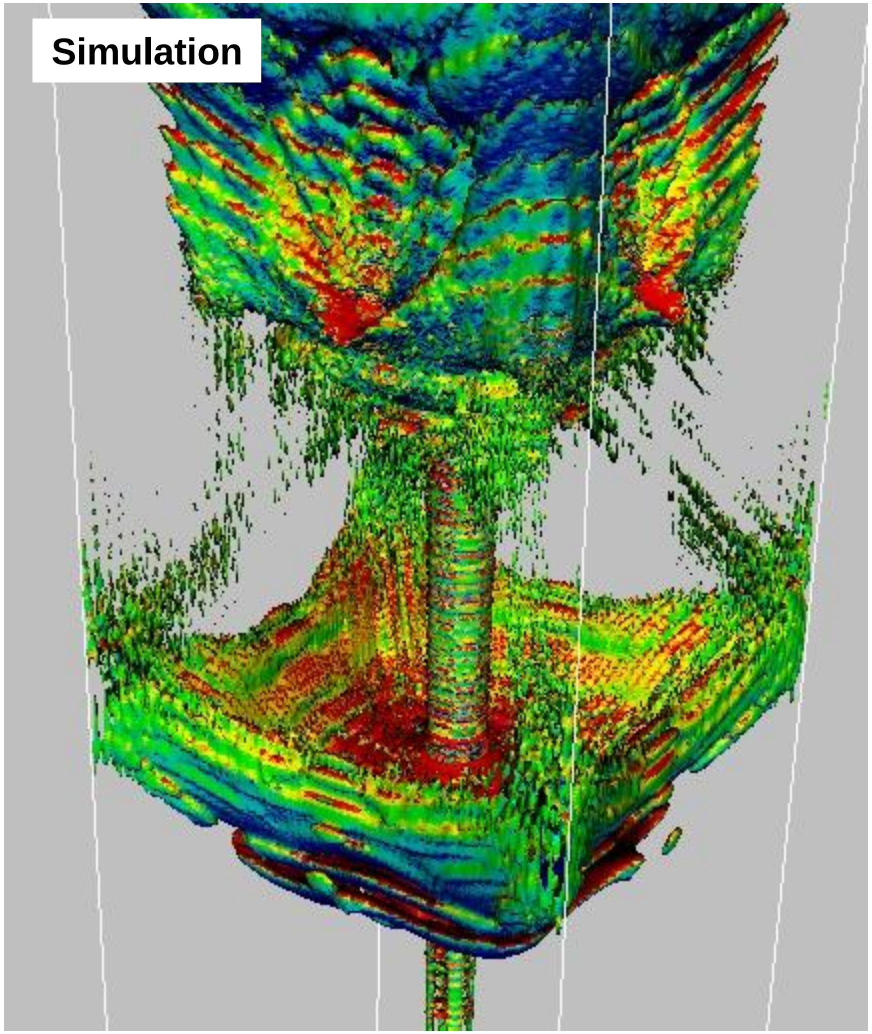

- objects with unknown symmetry
- crystallinity more complicated than cubic

⇨

Tomography (strain, shape, composition, …)
Strain in substrate

V.Holy *et al.*,

SXDM on a microelectronic device

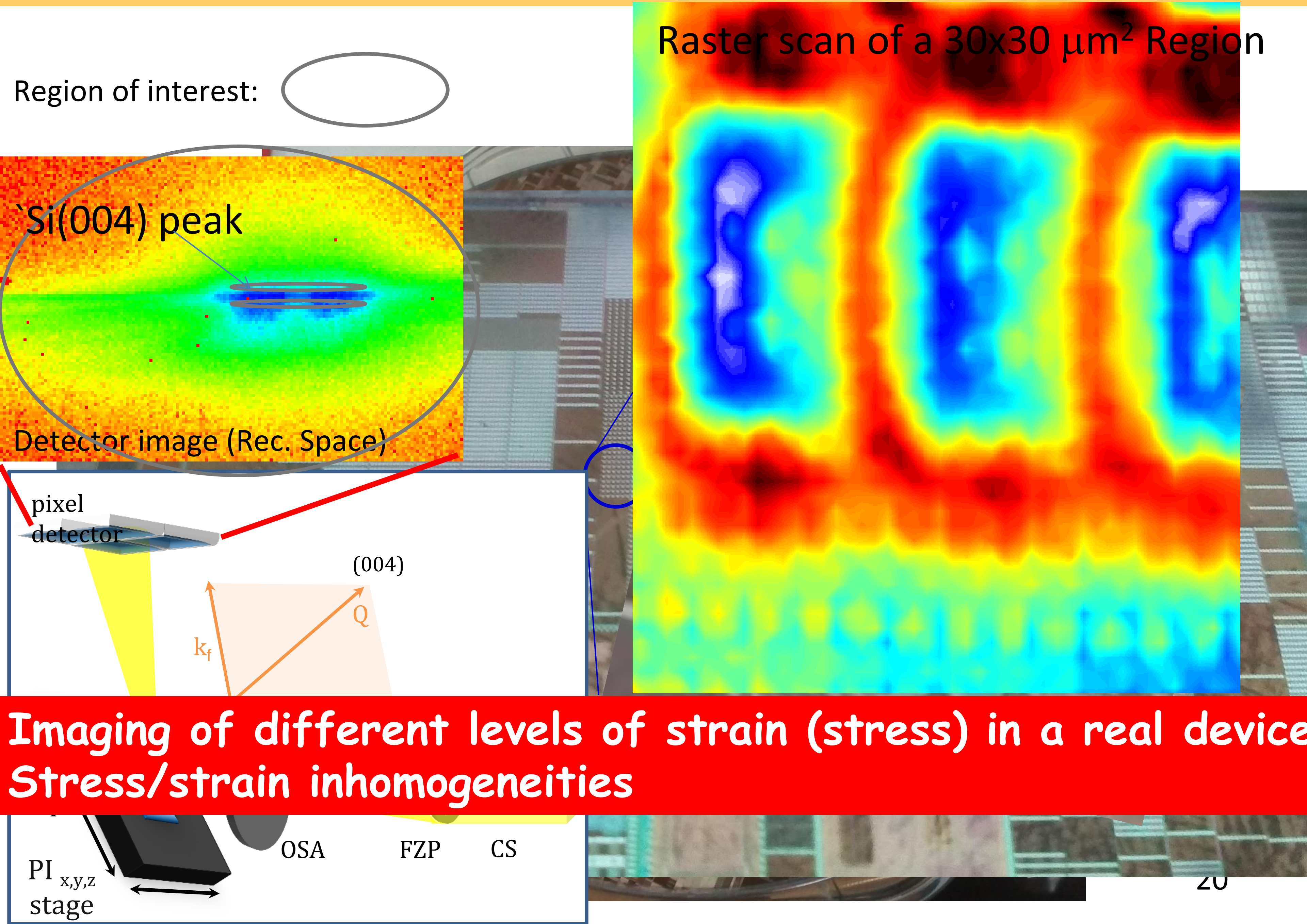

Imaging of different levels of strain (stress) in a real device

Stress/strain inhomogeneities

Scanning X-Ray Diffraction Microscopy
other example: high speed and high accuracy on strain

0.1mmx0.1 mm ESRF logo written in a Si crystal: imaging of lattice strain and tilt:

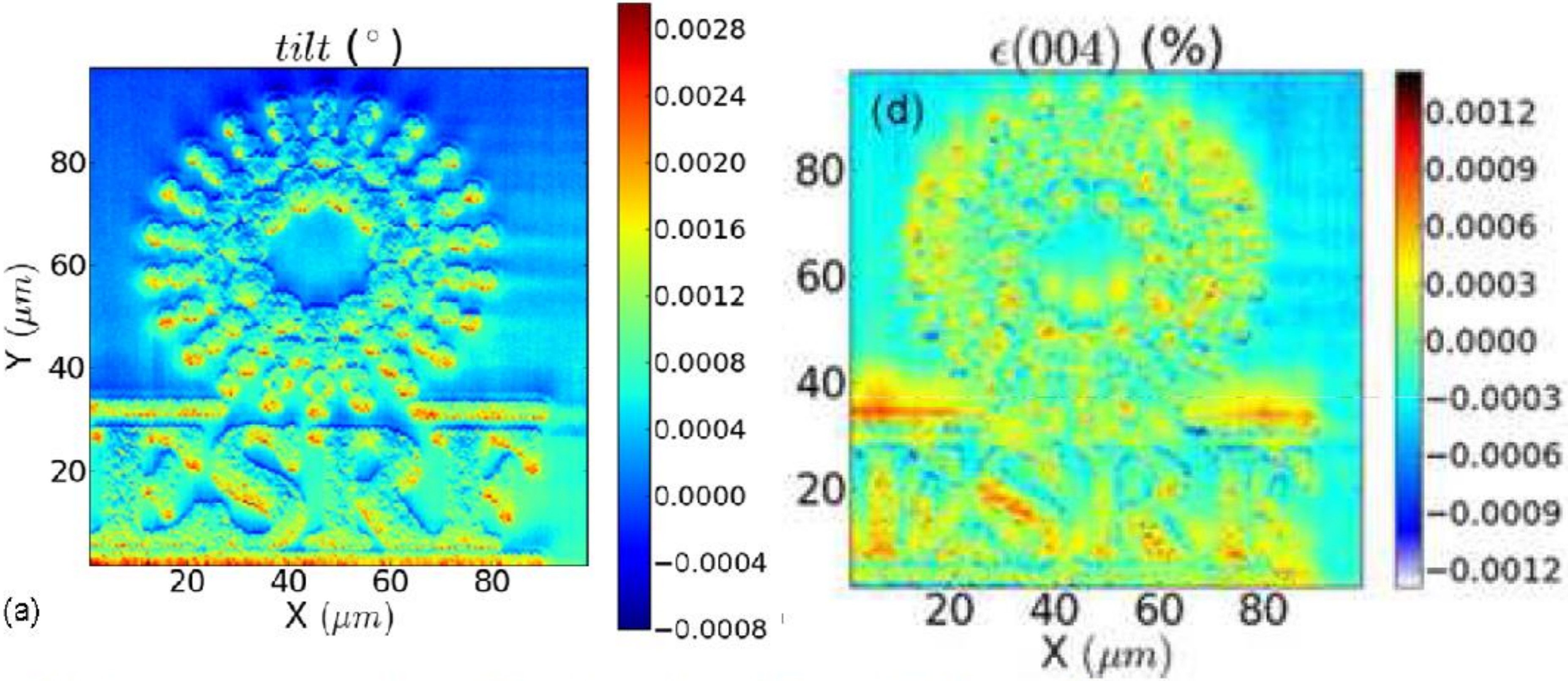

Relative strain levels of $\Delta a/a$ = few 10^{-6} can trace a landscape: We can “see” a ΔT of a few °C potentially in buried systems (working devices),

G. A. Chahine, M.-I. Richard, R. A. Homs-Regojo et al., *J. Appl. Cryst.* (2014)

3) Scanning Laue X-ray diffraction:

Scanning Laue Microdiffraction: principle

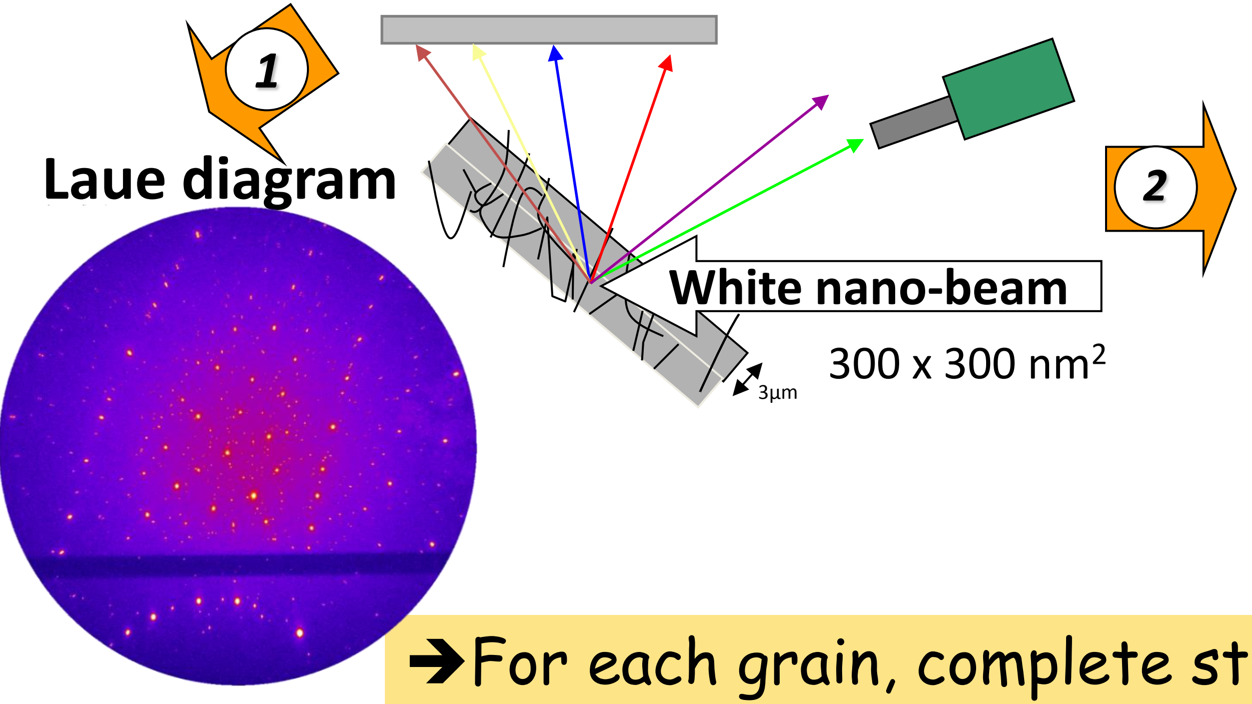

300 x 300 nm²

Energy sensitive detector

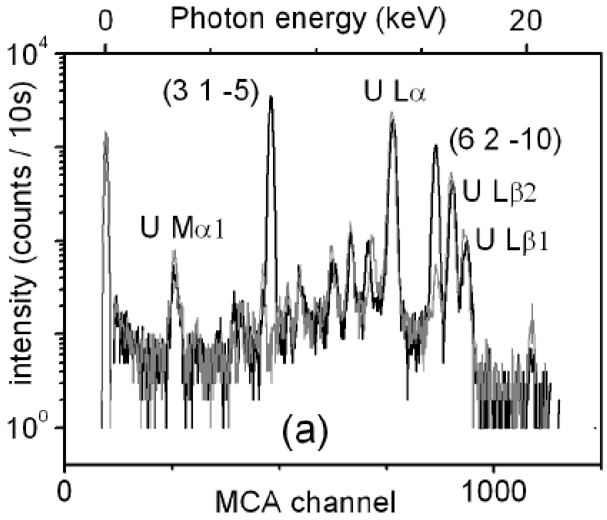

→ Scale of strain

→For each grain, complete strain tensor within 10^{-4}

Maps of

- → **Orientations**
- → **Strain** (10-4)
- → **Defects**

Orientation map

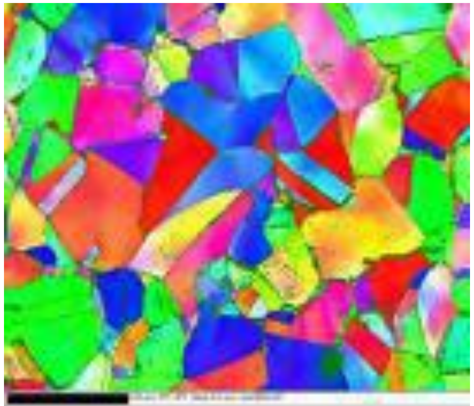

Strain map

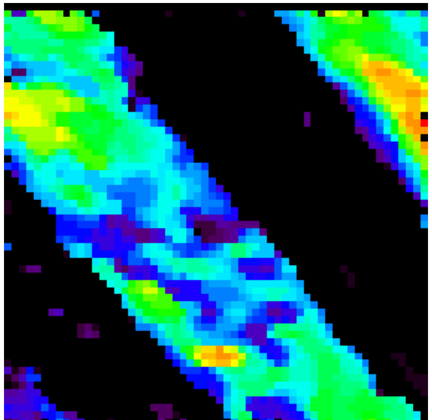

Fluorescence map

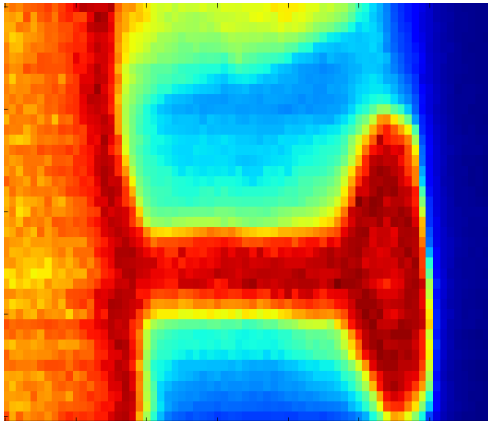

BM32 (ESRF)
Unique in Europe

4) Coherent X-ray Diffraction Imaging (CDI)

3D Coherent Diffraction Imaging (CDI)

goal: 3D reconstruction of shape and strain in single nanostructures

J. Miao *et al*, Nature **400**, 342 (1999)
I.K. Robinson *et al*, PRL **87**, 195505 (2001)
M. Pfeifer, *et al*., Nature **442**, 63 (2006)

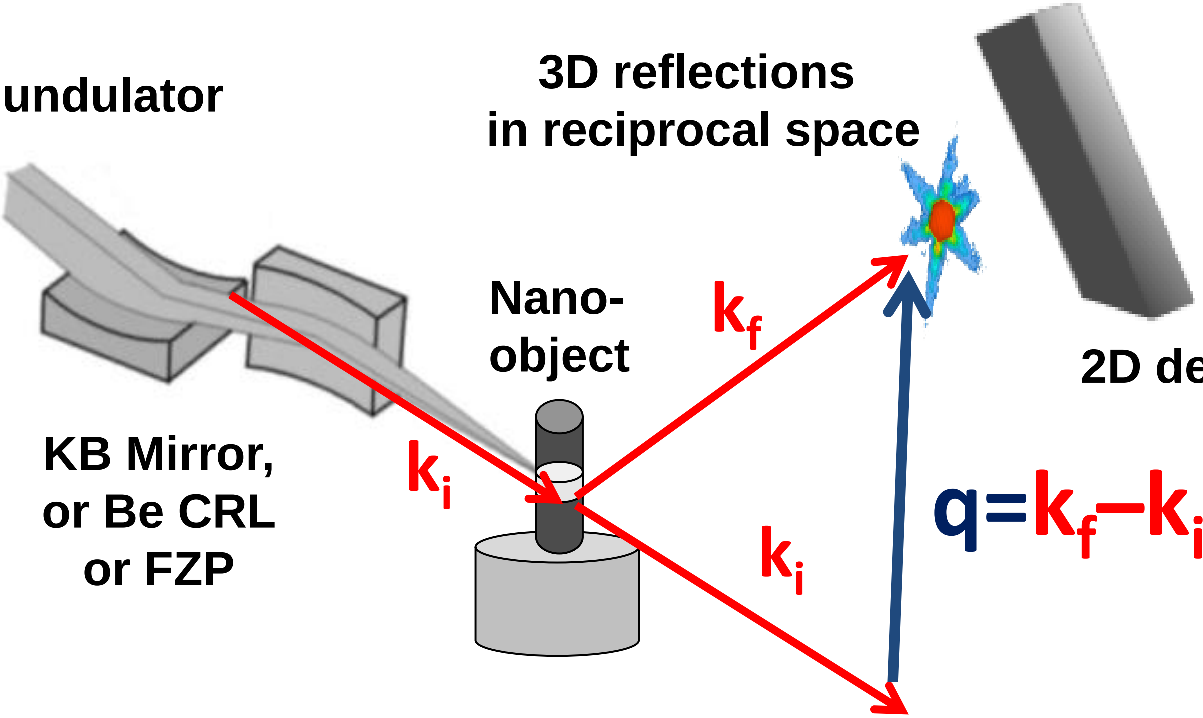

Synchrotron undulator X-ray beam

3D reflections in reciprocal space

Nano-object

2D detector

KB Mirror, or Be CRL or FZP

$$q = k_f - k_i = Q_{hkl}$$

- ***Synchrotron undulator monochromatic X-ray beam ➔ coherence length > 100 μm (transverse) and 1 μm (longitudinal)***
- ***Focusing optics ➔ focused coherent beam with 10^9-10^{10} ph/s in areas as small as 100x150 nm^2***

Basics of coherent diffraction imaging

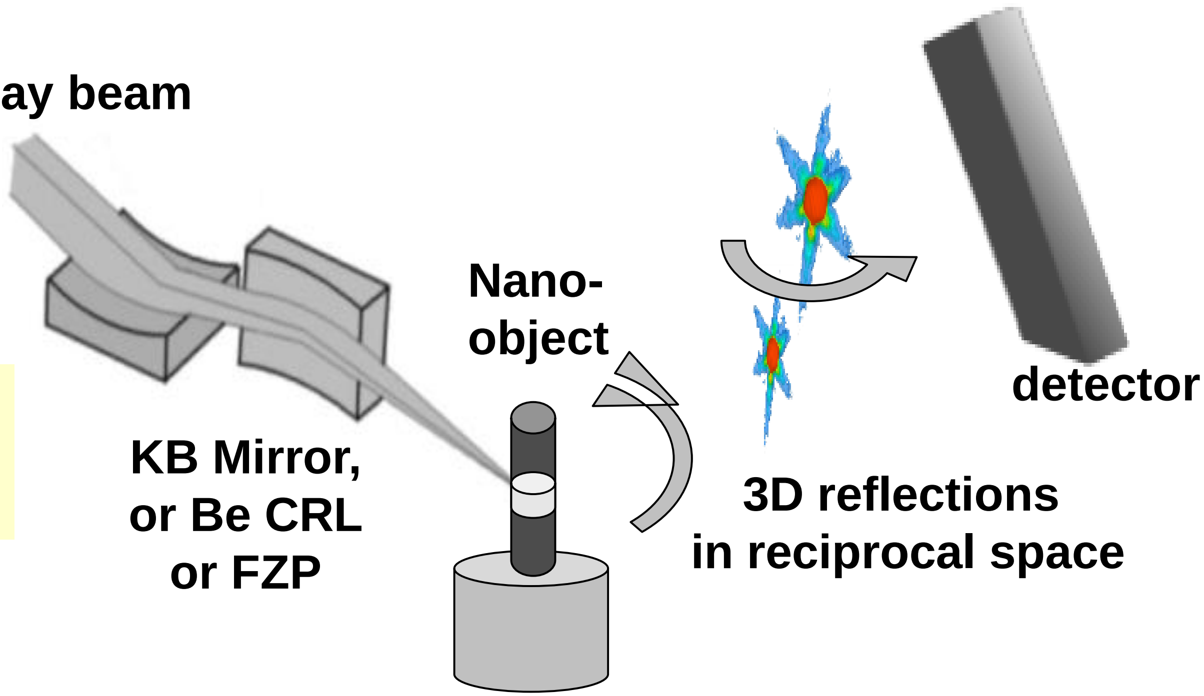

Take series of images on a Bragg peak

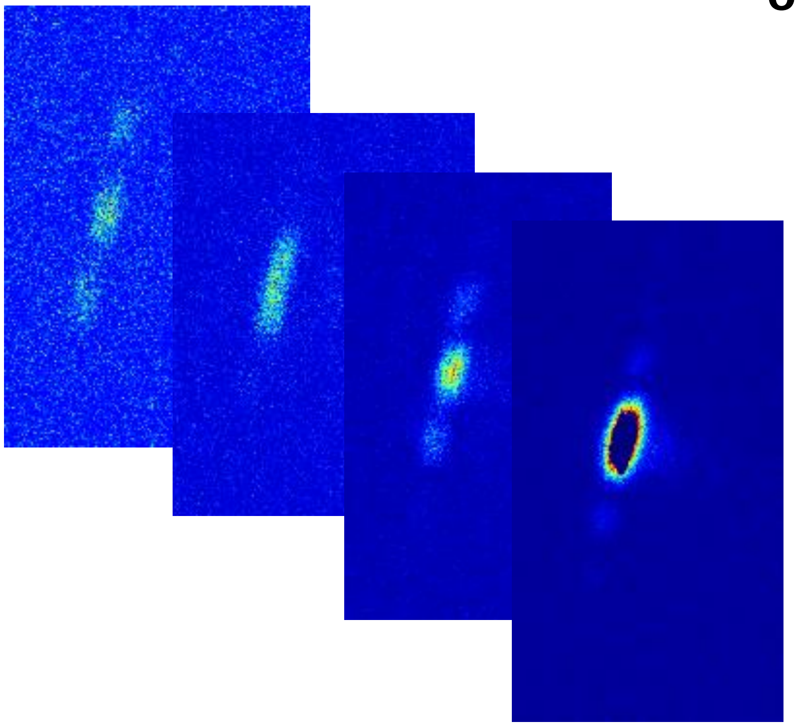

➔ Measure all 3D peak intensity

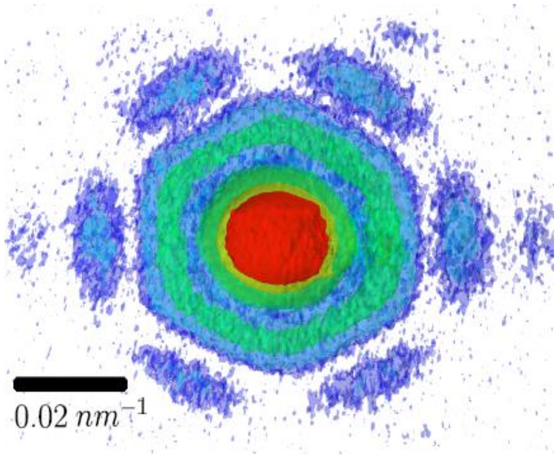

Movie

Basics of coherent diffraction imaging

InAs *nanowire Ø ~* ***150 nm***

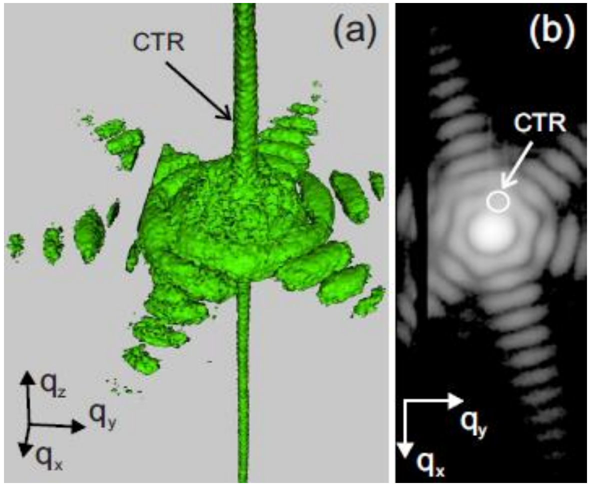

Si *nanowire Ø ~* ***95 nm***

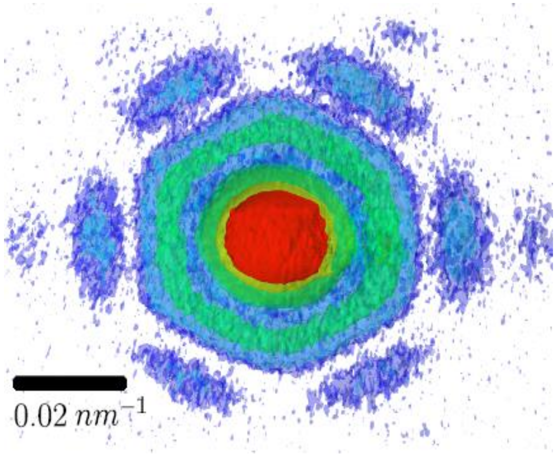

$$I(\mathbf{q}) \approx \left|FT[\rho(\mathbf{r})]\right|^2$$

FT

phase retrieval algorithm

FT

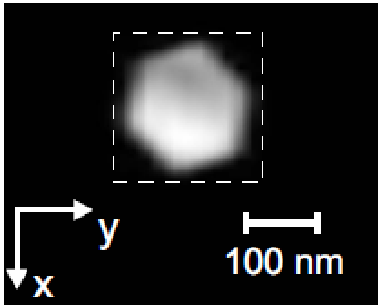

Reconstructed Object

resolution ~5 nm

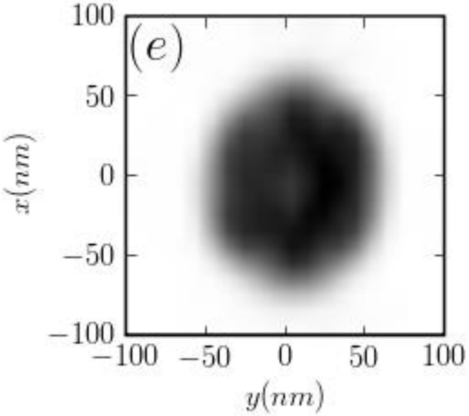

Phys. Rev. B 79, 125324 (2009)
Diaz et al

Phys. Rev. B 79, 195401 (2009)
Favre-Nicolin et al

Reconstruction iterative algorithm in a nutshell

- **Scattered intensity = square of FT of electron density**

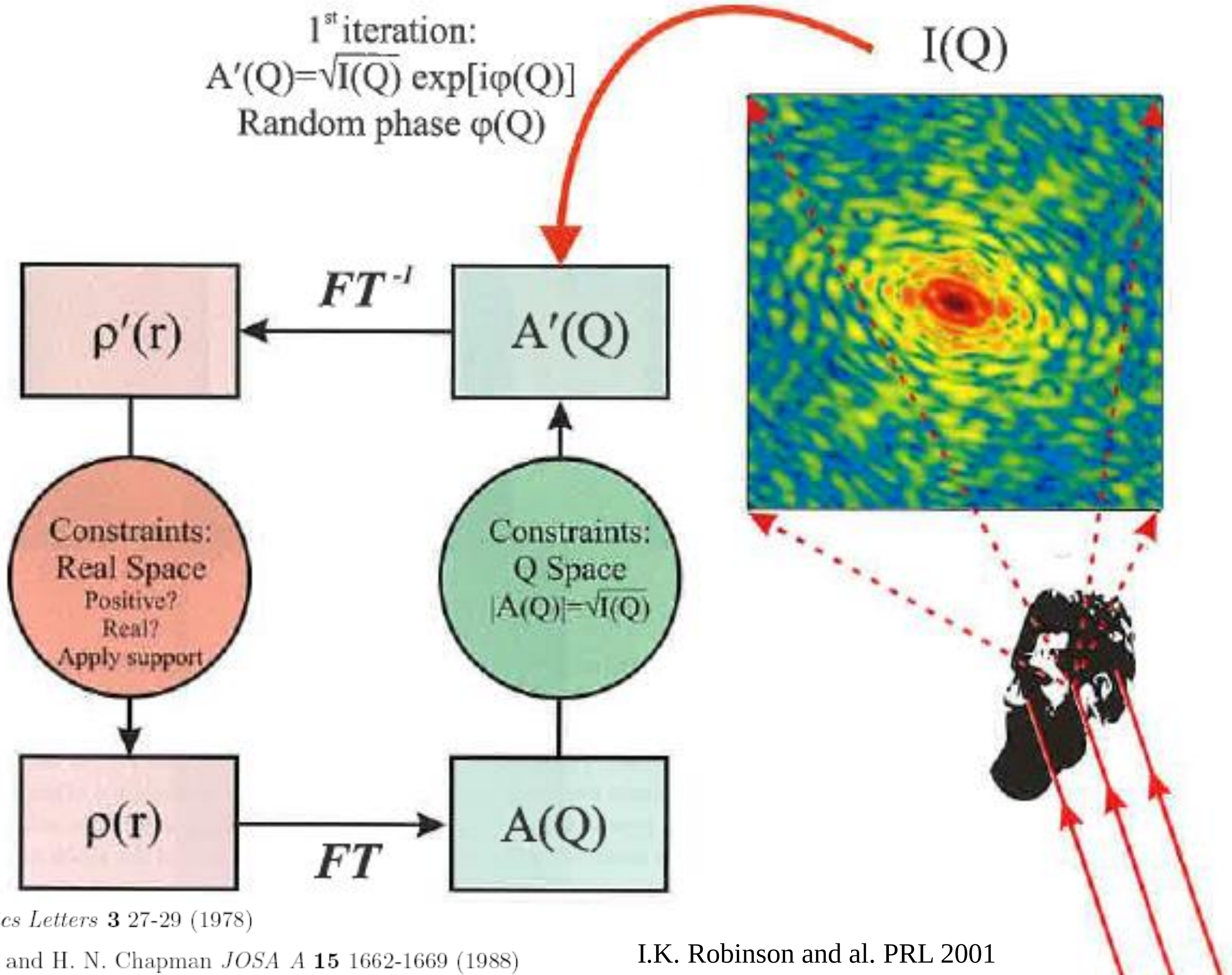

J. R. Fienup *Optics Letters* **3** 27-29 (1978)

J. Miao, D. Sayre and H. N. Chapman *JOSA A* **15** 1662-1669 (1988)

I.K. Robinson and al. PRL 2001

Needs oversampling (at least twice the Nyquist frequency)

So far for the shape, but what about the strain ?

- Scattered intensity = square of FT of electron density

$$I(q) = |A(q)|^2 \qquad A(q) = \int \rho(\mathbf{r}) \exp(\mathrm{i}\mathbf{q}\cdot\mathbf{r})\mathrm{d}\mathbf{r}$$

- In a crystal with lattice r_n + strain field $u(r_n)$:

$$\rho'(\mathbf{r}) = s(\mathbf{r}) \sum_{n=1}^{N} \delta(\mathbf{r} - \mathbf{r}_n - \mathbf{u}(\mathbf{r}_n)) \,,$$

s(r) = shape of crystal

$$A(q) = A\hat{s}(\mathbf{q}) * \sum_{n=1}^{N} \exp(\mathrm{i}\mathbf{q}\cdot(\mathbf{r}_n + \mathbf{u}(\mathbf{r}_n)))$$

- Close to a Bragg peak $\mathbf{q} = \mathbf{Q}_{hkl} + \mathbf{q}'$

$$A(q') \approx \int \rho'(\mathbf{r}) \exp(\mathrm{i}\mathbf{q}'\mathbf{r})\mathrm{d}\mathbf{r}$$

FT of an effective electron density

$$\rho'(\mathbf{r}) = \rho(\mathbf{r}) \exp \mathrm{i}(\mathbf{Q}_{hkl}\cdot\mathbf{u}(\mathbf{r}))$$

Electron density
modified by strain field u(r)

Amplitude ➔ *ρ(r)* ➔ shape
Phase ➔ Q_{hkl}.u(r) ➔ projection of strain field along Q_{hkl} direction

Ex: Diffraction by a small hexagonal crystal

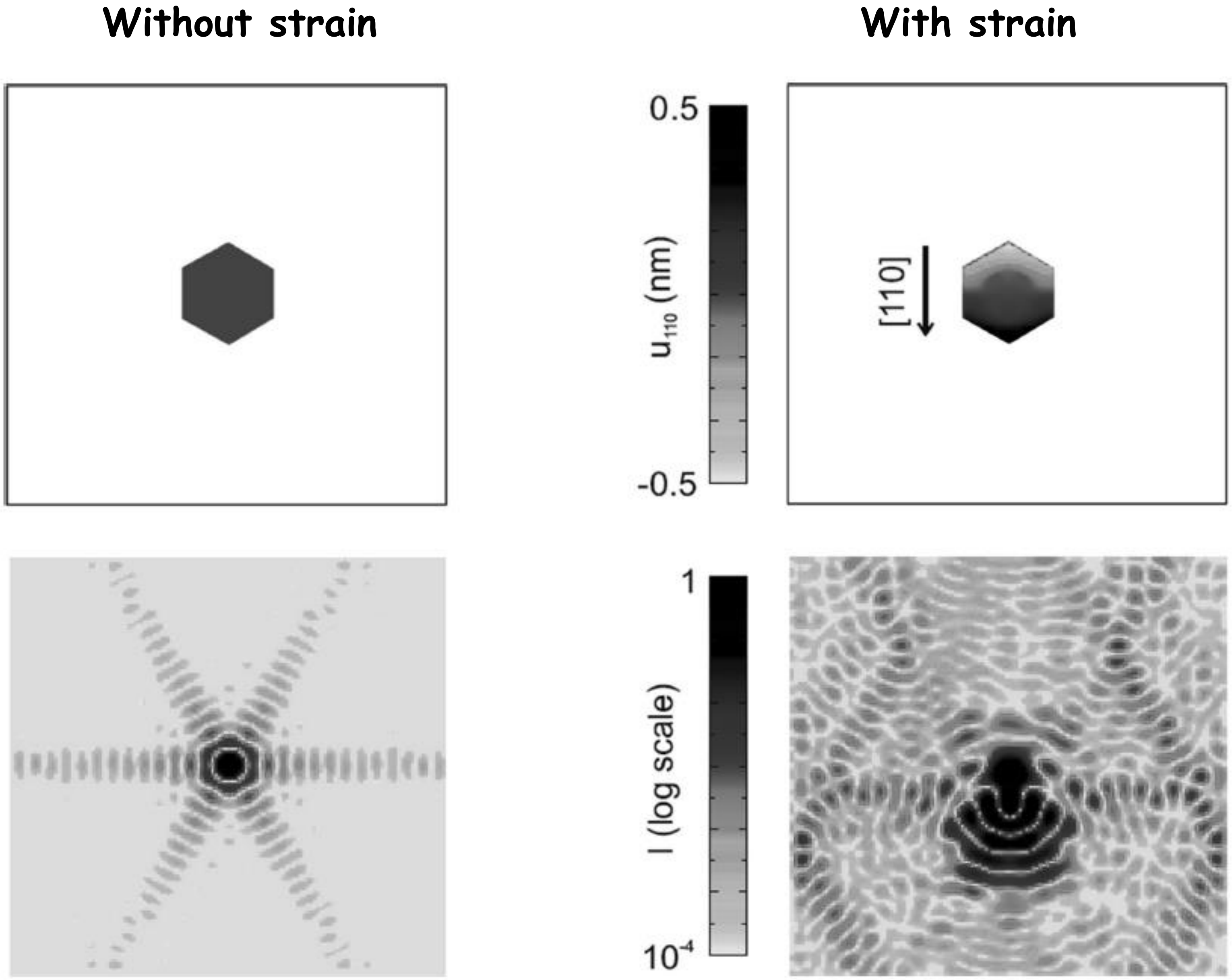

Without strain

With strain

2D reconstruction of strain in CDI?

$$\boxed{A(\mathbf{q}) \approx FT\left[s(\mathbf{r})\, e^{2i\pi \mathbf{Q}_{hkl}\,\cdot\,\mathbf{u}(\mathbf{r})}\right]}$$

Sensitivity to strain needs high $\mathbf{Q}_{hkl}$ values

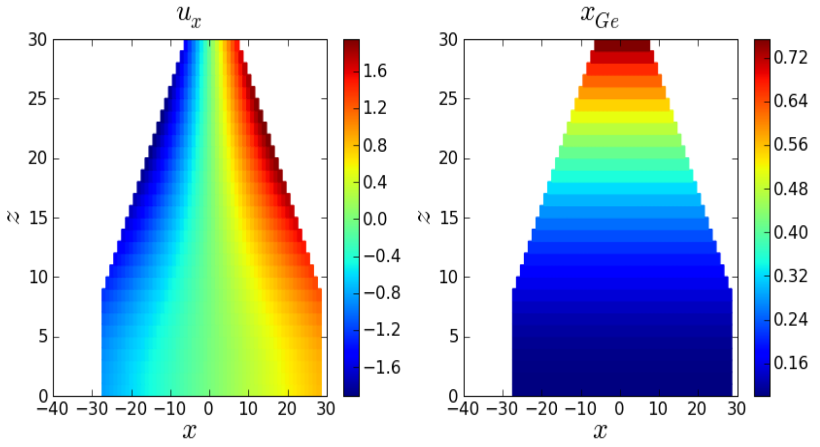

Simulated Si/Ge 30nm nano-rocket

- *increased Ge concentration with z*
- *relaxation with z*

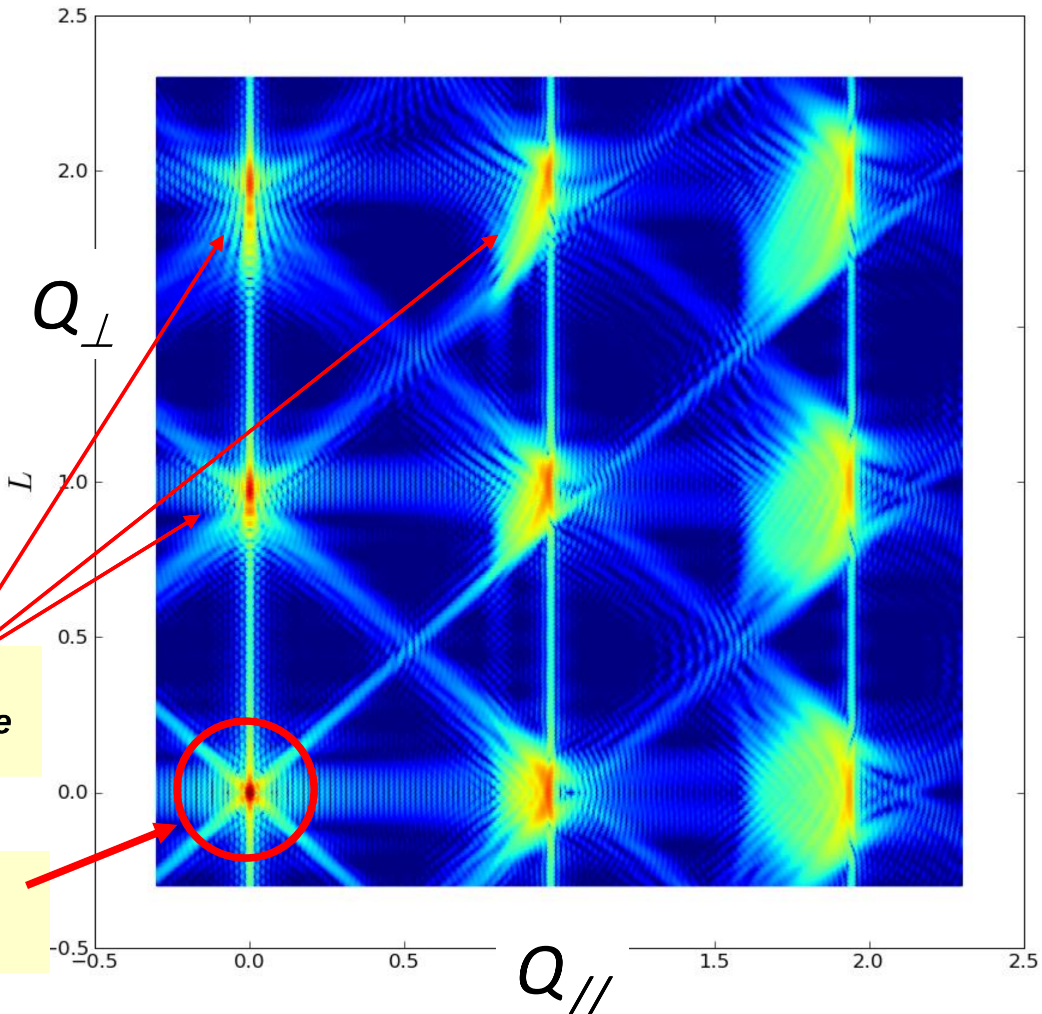

Bragg : sensitive to the shape, density profile and strain

SAXS : sensitive to The shape & density profile

Example of 3D reconstruction of the full strain tensor in a ZnO nanorod using 6 Bragg reflections

$$A(\mathbf{q}) \approx FT\left[s(\mathbf{r})e^{2i\pi \mathbf{Q}_{hkl}\boxed{.\mathbf{u}(\mathbf{r})}}\right]$$

Measuring the CDI on 6 independent reflections

Reconstruct the full 3D displacement field inside the nanocrystal

➔ ***Full strain tensor in a single nanostructure***

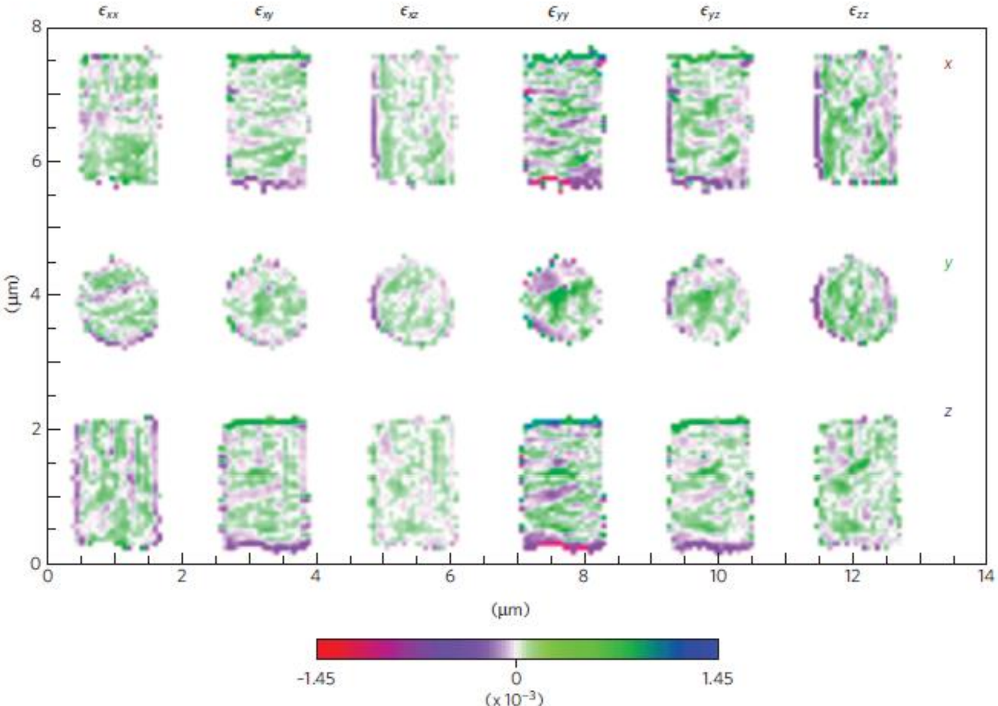

Newton et al., Nat. Mater. ***9*** *(2010), 120 - 124*

Other model-free techniques to image the shape and the internal atomic structure (strain) of nanoobjects

5) Fourier Transform Bragg holography

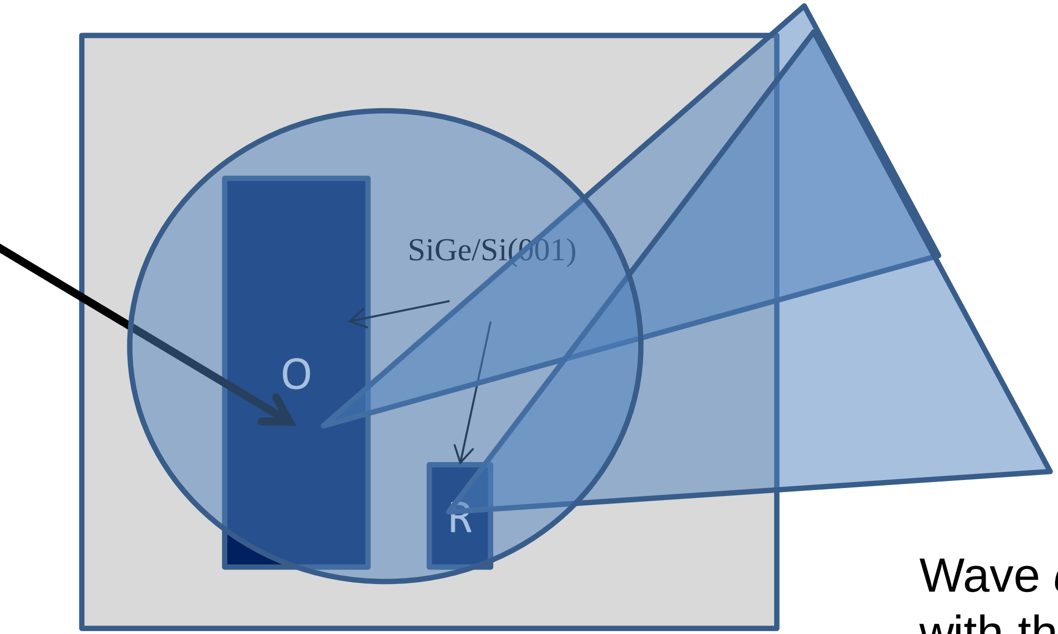

Wave *diffracted* by the object (O) interferes with the wave *diffracted* by the reference crystal (R) (same Bragg angle)

➔ Recover the phase by direct Fourier Transform!

Chamard. *PRL* **104**, 165501 (2010), Sci. Rep. **5**, 9827 (2015)

Fourier Transform Bragg holography

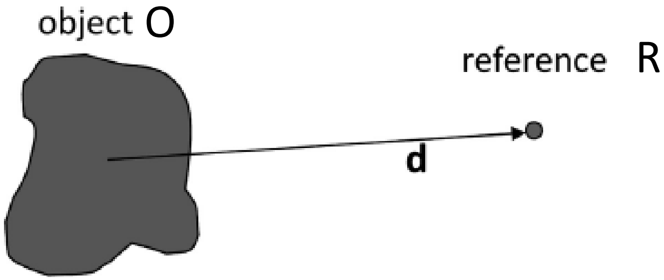

$$I(\mathbf{q}) = \left|A_O(\mathbf{q}) + A_R(\mathbf{q})\right|^2$$

$$TF(I)^{-1} = f_O(r)\otimes f_O(r)^* + f_R(r)\otimes f_R(r)^* + f_O(r)\otimes f_R(r)^* + f_R(r)\otimes f_O(r)^*$$

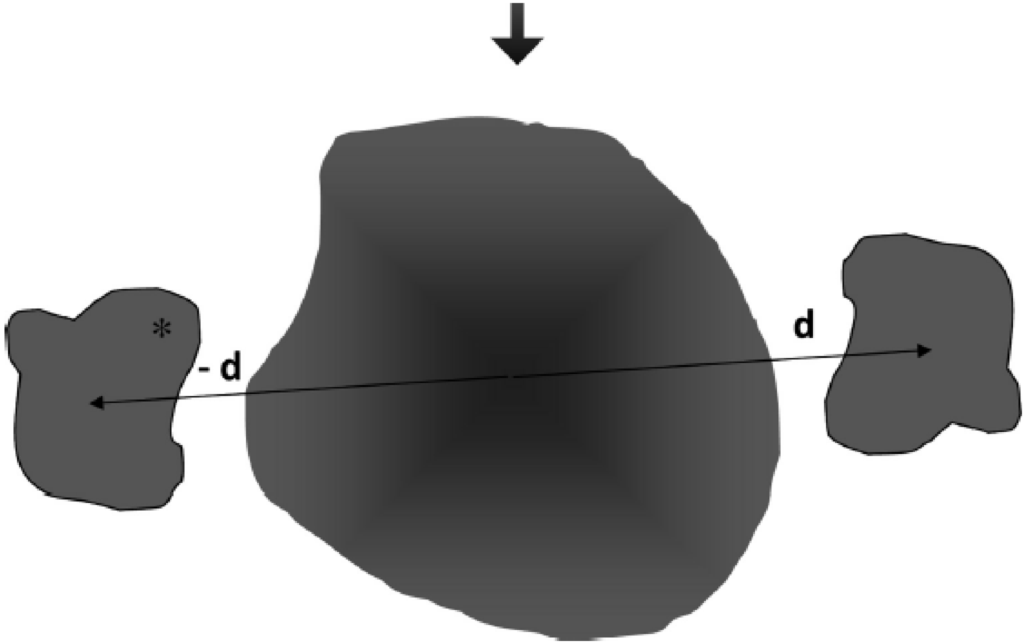

X-ray Bragg holography: A 3D look inside nanostructures

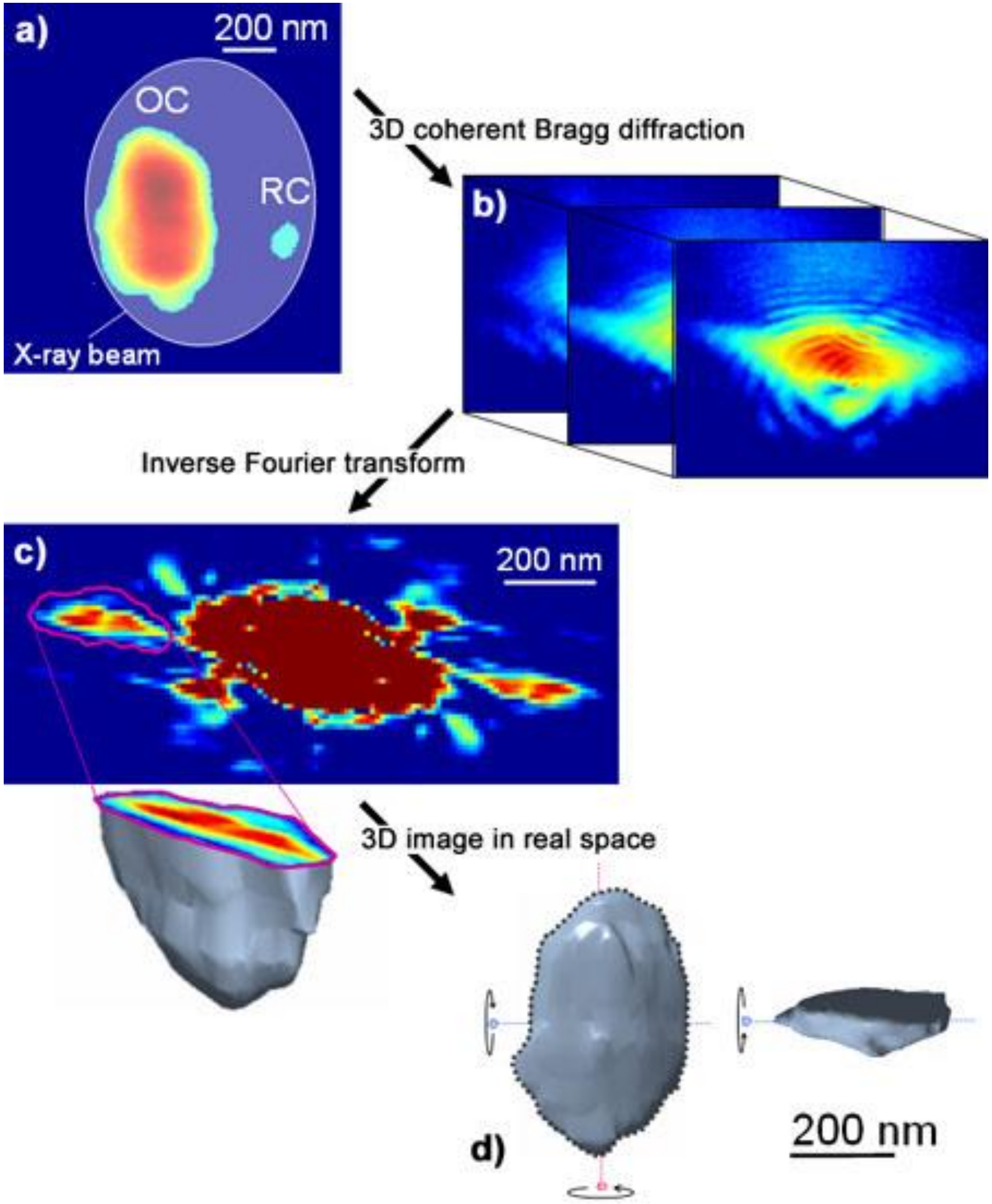

Other model-free techniques to image the shape and the internal atomic structure (strain) of nanoobjects

6) Bragg Ptychography

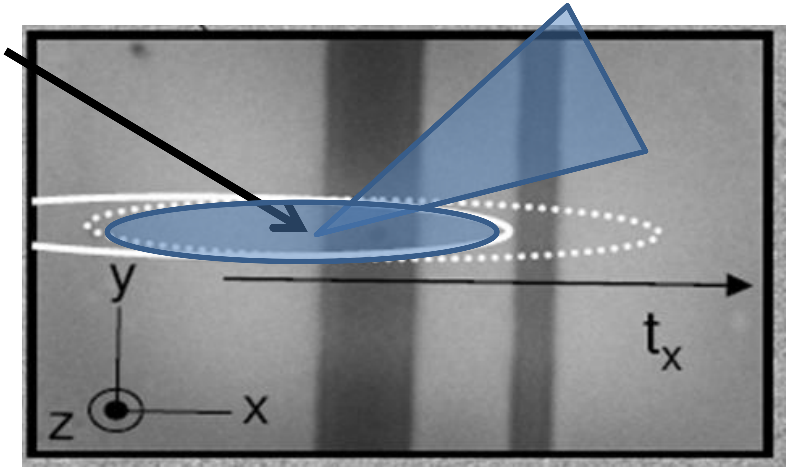

Redundancy of information from overlapping areas makes retrieval algorithm very robust

➔ **Recover the phase**

Godard *Nature Com.* Nov 2011

Principle of iterative ptychography algorithm

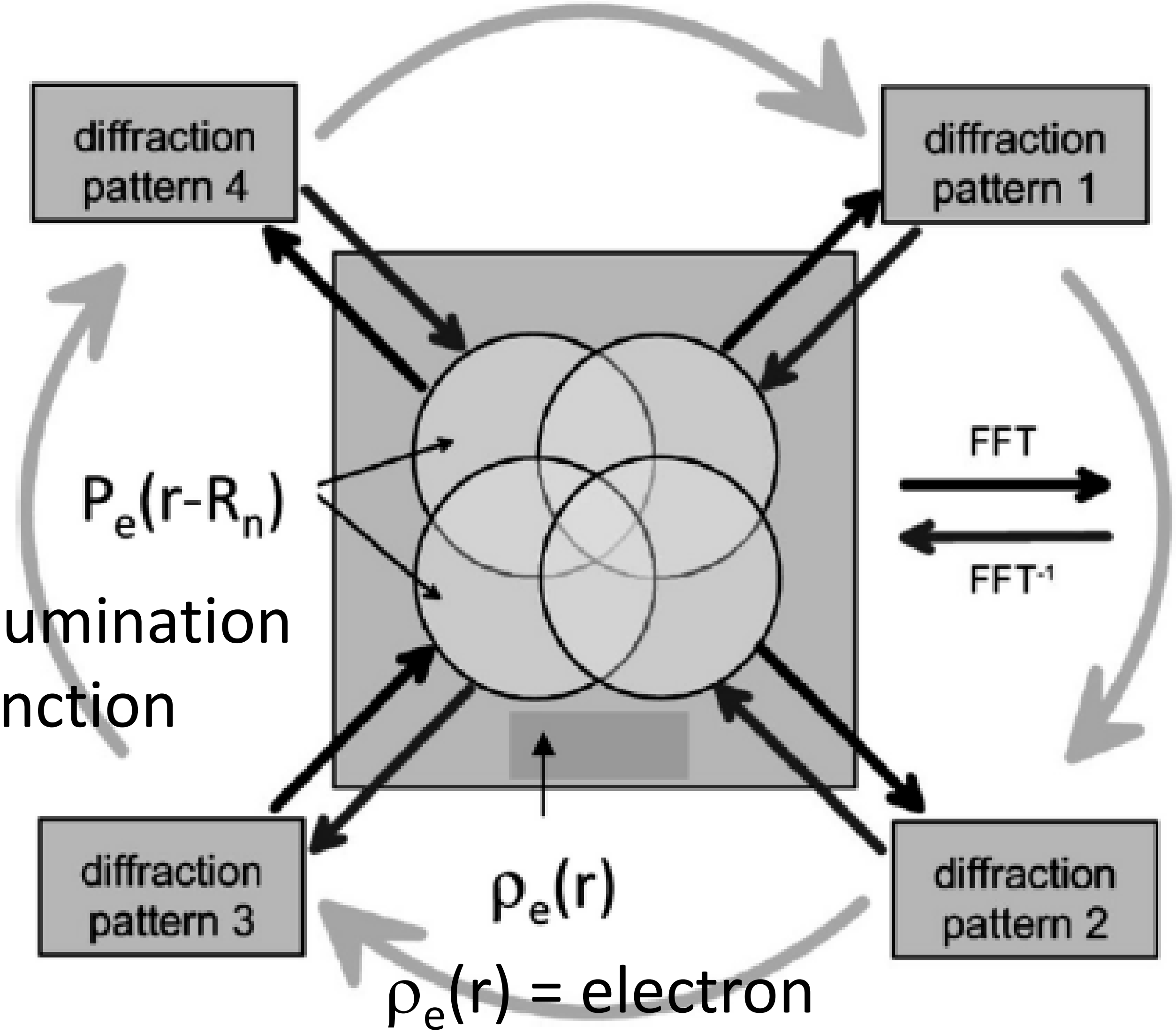

$P_e(r)$ = Illumination function

$\rho_e(r)$ = electron density

3D ptychography: image reconstruction without hypothesis

Ex: 3D reconstruction of a mouse bone internal structure displaying osteocyte lacuna (L) & connecting canaliculi (C)

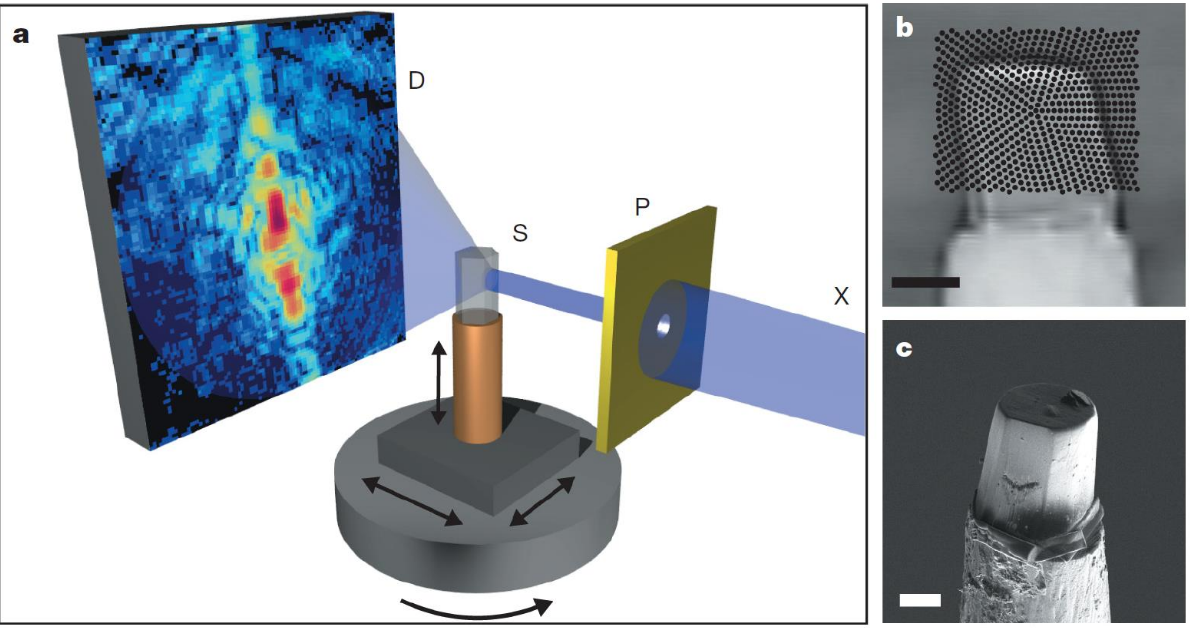

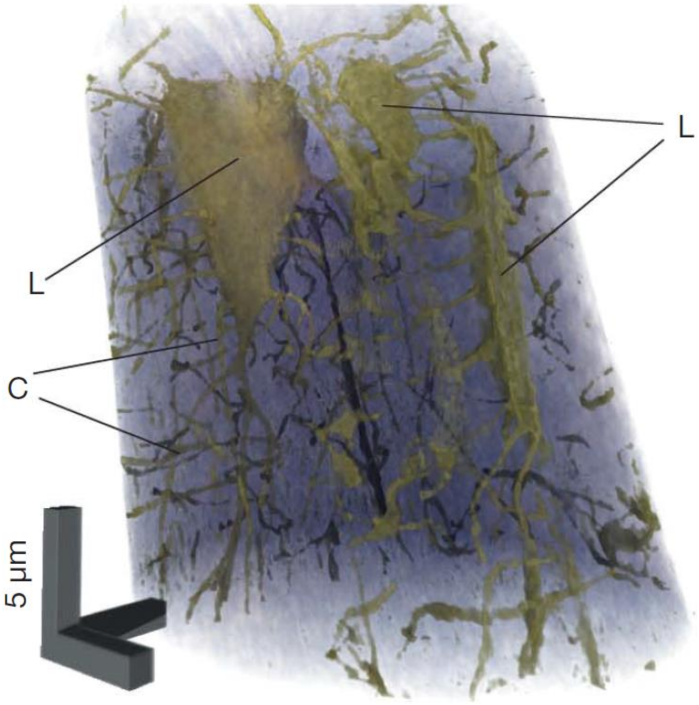

Voxel size: 65 nm
Resolution: ~120 nm
Dose: ~2MGy

M. Dierolf et al
467 Nature (2010) 436

Some perspectives of X-ray diffraction on unique objects

Full characterization of active devices

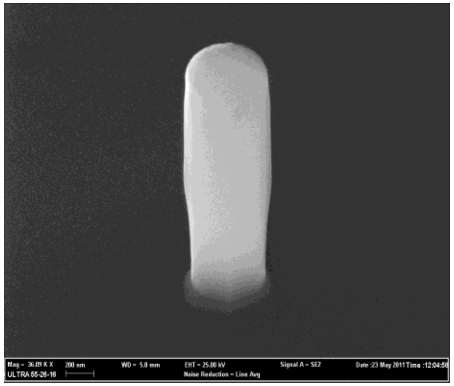

Photonic nanowire: InAs QDs in GaAs
=>locate the QD, correlate with photoemission properties (efficiency, polarisation,...

V. Favre-Nicolin et al

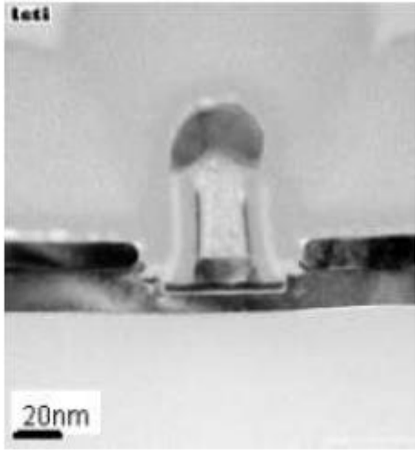

n-MOSFET FDSOI
Study strain distribution vs conductivity

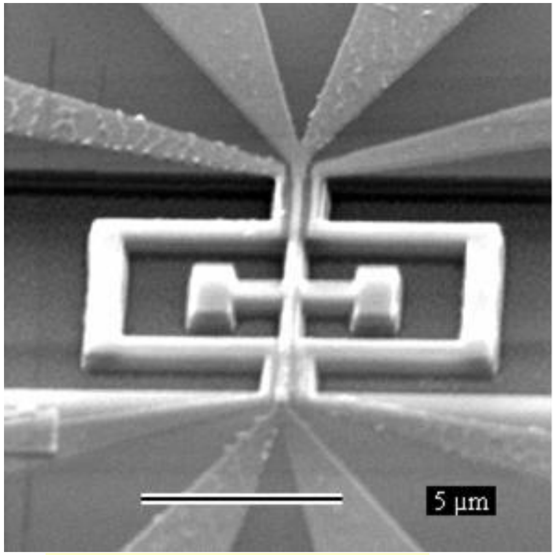

NEMS
Time-resolved strain

In 5 years, routine reconstructions of single objects with a 0.2 nm resolution and a sub-Å resolution for atomic displacements in 3D.

Key ongoing developments :
- *Measure multiple reflections for a single object (full strain)*
- *Correlation with physical properties on same objects*
- *In situ/in operando analysis*
- *Time resolved (XFEL)*

Pump-probe experiments

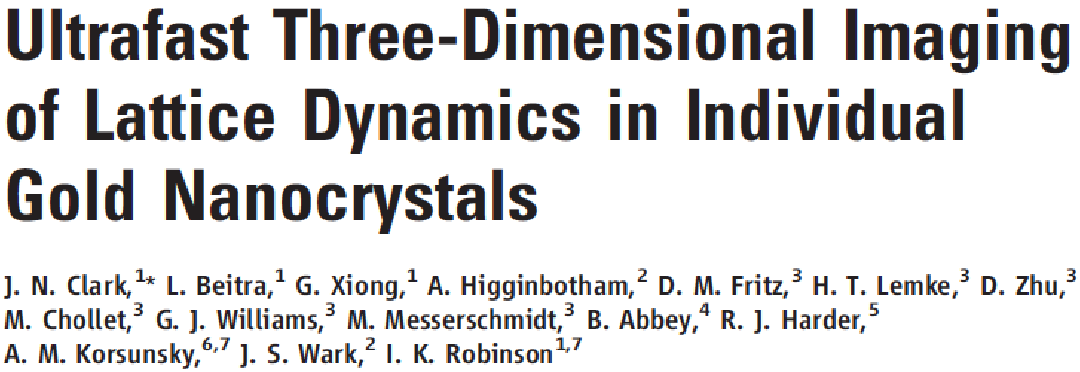

Ultrafast Three-Dimensional Imaging of Lattice Dynamics in Individual Gold Nanocrystals

J. N. Clark,[1*] L. Beitra,[1] G. Xiong,[1] A. Higginbotham,[2] D. M. Fritz,[3] H. T. Lemke,[3] D. Zhu,[3]
M. Chollet,[3] G. J. Williams,[3] M. Messerschmidt,[3] B. Abbey,[4] R. J. Harder,[5]
A. M. Korsunsky,[6,7] J. S. Wark,[2] I. K. Robinson[1,7]

Science **341,** 51-59 (2013)

Free Electron Lasers:
- **Based on Linear Accelerators**
- **Deliver ultrashort pulses (< 100 fs = 0.1 ps= 10^{-13} s)**
- **(Transversely) Spatially coherent (laser-like) radiation**

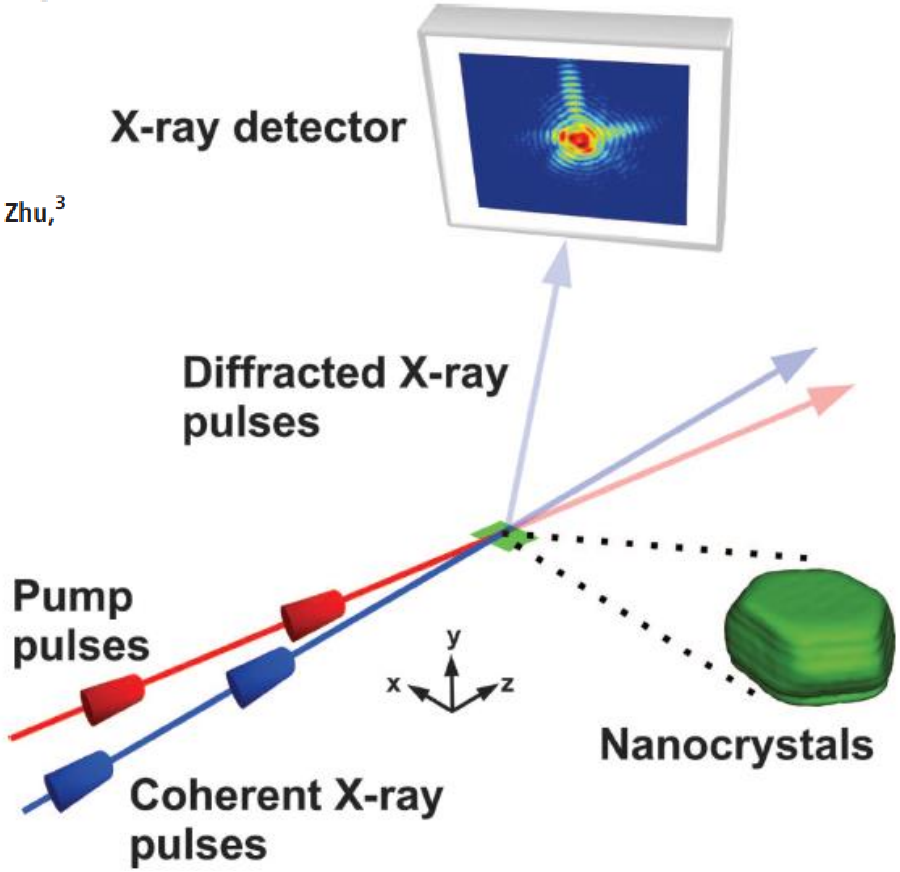

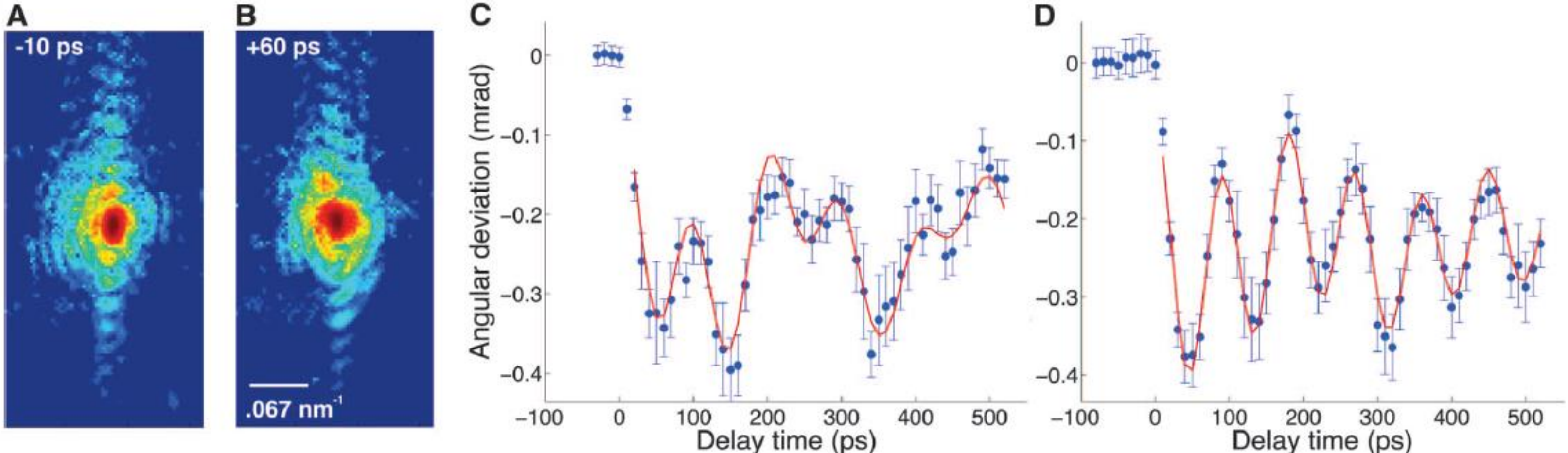

Imaging of vibrational modes

Beyond the analysis of the Bragg spots position: imaging of vibrations: acoustic phonons in a gold nanocrystal

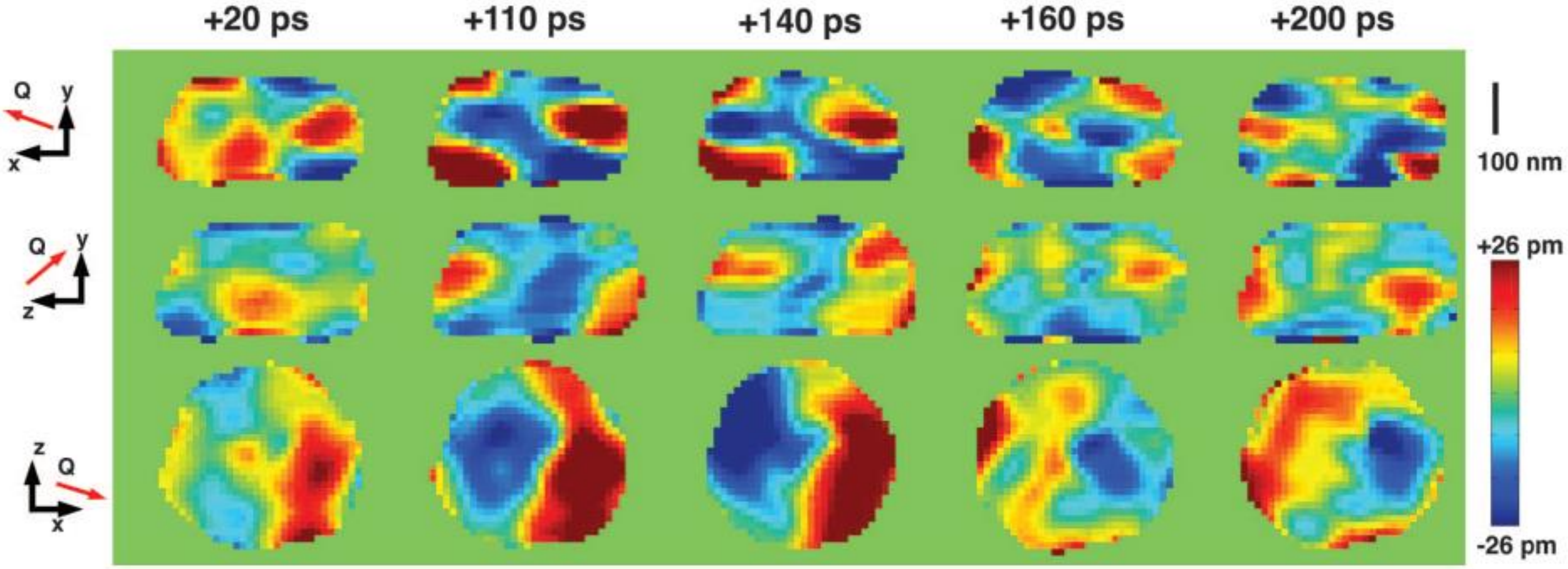

In the near future: time resolution < 10 fs and spatial resolution < 5 nm.

Very diverse applications of diffractive imaging methods with coherent x-rays in physical science

CDI on molten Fe-rich alloy
+ crystalline
Olivine at 6 GPa and 1800°C
Mimicking earth upper
mantle

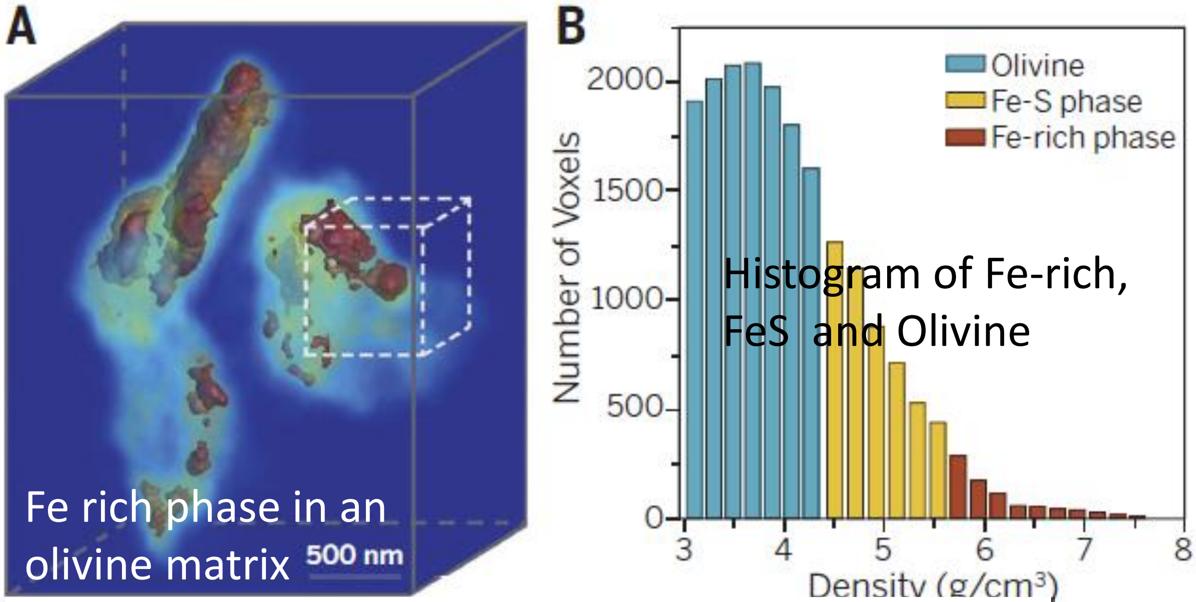

Fe rich phase in an olivine matrix

Histogram of Fe-rich, FeS and Olivine

Reconstruction of
LiFePO4 nanoplate (used
(for electrochemical
energy storage)
combining ptychography
and anomalous
scattering at Fe K edge

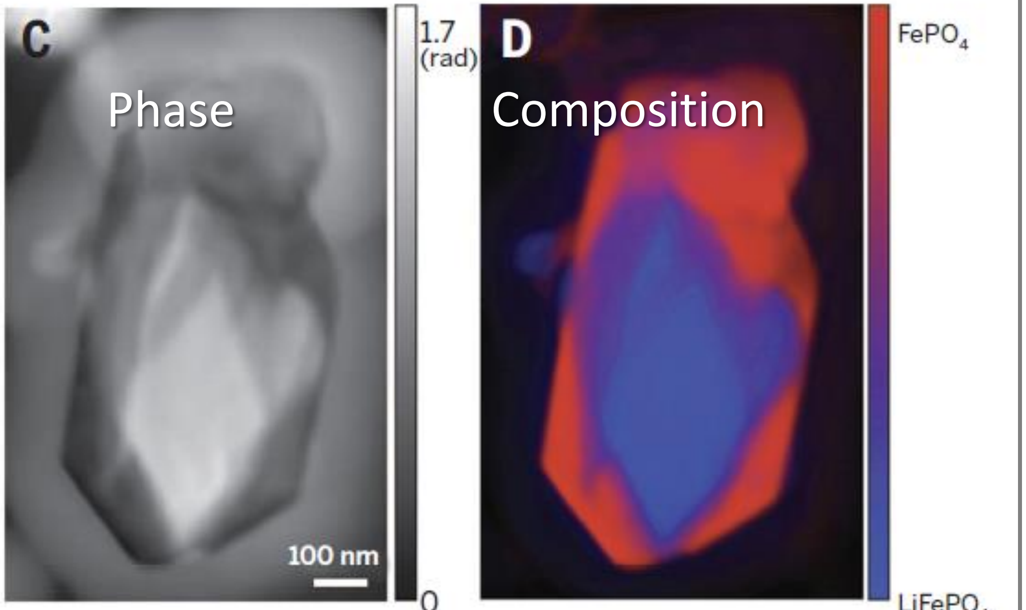

Phase

Composition

Very diverse applications of diffractive imaging methods with coherent x-rays in life science

Unstained yeast pore cell

Humain chromosome

Herpes virus virion

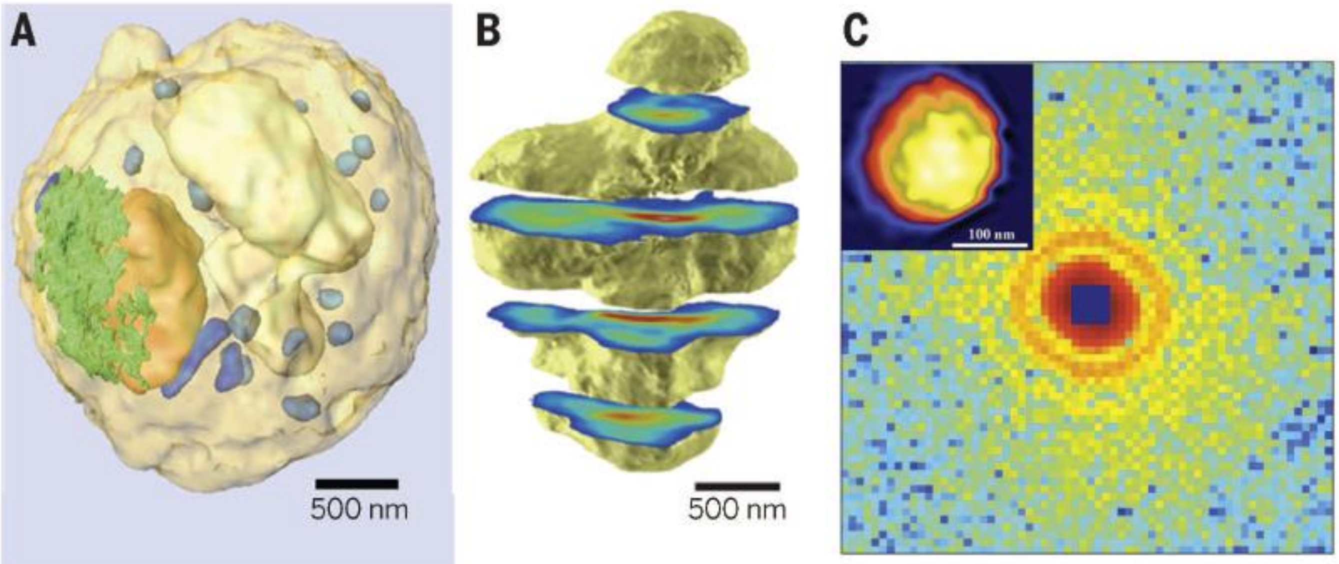

CDI of giant mimivirus particle (XFEL)

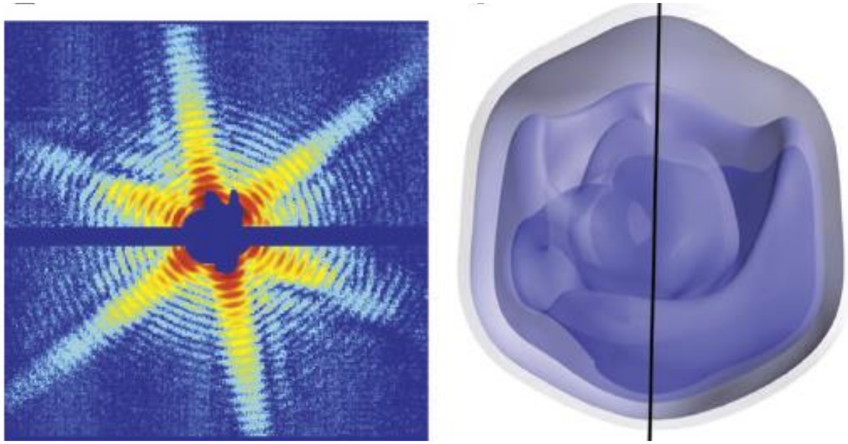

ent x-rays. (**A**) 3D mass density distribution of a whole, unstained yeast spore cell, showing nucleus (orange), endoplasmic reticulum (green), vacuole (white), mitochondria (blue), and granules (light blue) (*44*). (**B**) 3D image of an unstained human chromosome where the highest electron density is around the centromere (in red) (*46*). (**C**) First coherent x-ray diffraction pattern measured from a single, unstained herpesvirus virion and its reconstructed structure (inset), where the capsid is in yellow (*47*). (**D**) Quantitative 3D measurements of the osteocyte lacunae (L) and the connecting canaliculi (C) in a bone matrix (*15*). (**E**) A representative diffraction pattern of a giant mimivirus particle collected with a single

LCLS pulse, where the symmetry of the diffraction pattern is clearly visible (*16*). (**F**) 3D structure of the mimivirus reconstructed from 198 diffraction patterns with higher density in blue and lower density in white (*50*). The vertical line represents the pseudo-fivefold axis. (**G**) Coherent x-ray diffraction pattern collected from a

Some conclusions

- ***Scanning X-ray fluorescence***
  - *3D nanotomography of composition with nm resolution*
- ***Scanning X-ray diffraction microscopy***
  - *(in)homogeneity of strain/rotations in real devices*
- ***Micro-Laue diffraction**:*
  - *Fast study of single nano-objects/grains*
  - *2D/3D strain determination*
- ***Coherent Bragg Imaging / Holography / Ptychography**:*
  - *Reconstruct objects smaller than 100 nm with resolution down to 2 nm in 2D and 5.5 nm in 3D.*
  - *Stacking fault structure / individual defects*
  - *Deformation field (2D/3D) with sensitivity down to ~0.05 nm*
  - *Towards heterogeneous materials*

- ***Future sources = X-ray Free Electron Lasers (XFEL)***
  - *Even higher resolution + time-resolved down to ps.*

A few references

General references:

“Elements of Modern X-Ray Physics” 2nd edition
Jens Als-Nielsen & Des McMorrow WILEY 2011

Nanobeam/CDI/Ptychography/holography:

“Nanobeam X-Ray Scattering: Probing Matter at the Nanoscale”, J. Stangl, C . Mocuta, V. Charmard and D. Carbone, WILEY-VCH (2014)

Coherent diffraction / holography / ptychography:

- J. Miao *et al*, Nature **400**, 342 (1999)
- I.K. Robinson *et al*, PRL **87**, 195505 (2001)
- M. Pfeifer, *et al*., Nature **442**, 63 (2006)
- G.J. Williams *et al*., PRL **90**, 175501 (2003)
- M.A. Pfeifer et al., Nature 442, 63 (2006)
- I. Robinson and R. Harder, Natur. Mater. 8, 291 (2009)
- Nat. Mater. **9** (2010), 120; Nature **463** (2010), 214
- G. Ice et al., Science **334**, 1234 (2011)
- W. Yang et al, Nature comm. **4**:1680 (2013)
- J.N. Clark et al., Science **341**, 56 (2013)

French CRG/IF BM32 Beamline @ ESRF

Nanostructures, Surfaces, Interfaces by X-ray scattering

/www.esrf.eu/UsersAndScience/Experiments/CRG/BM32/

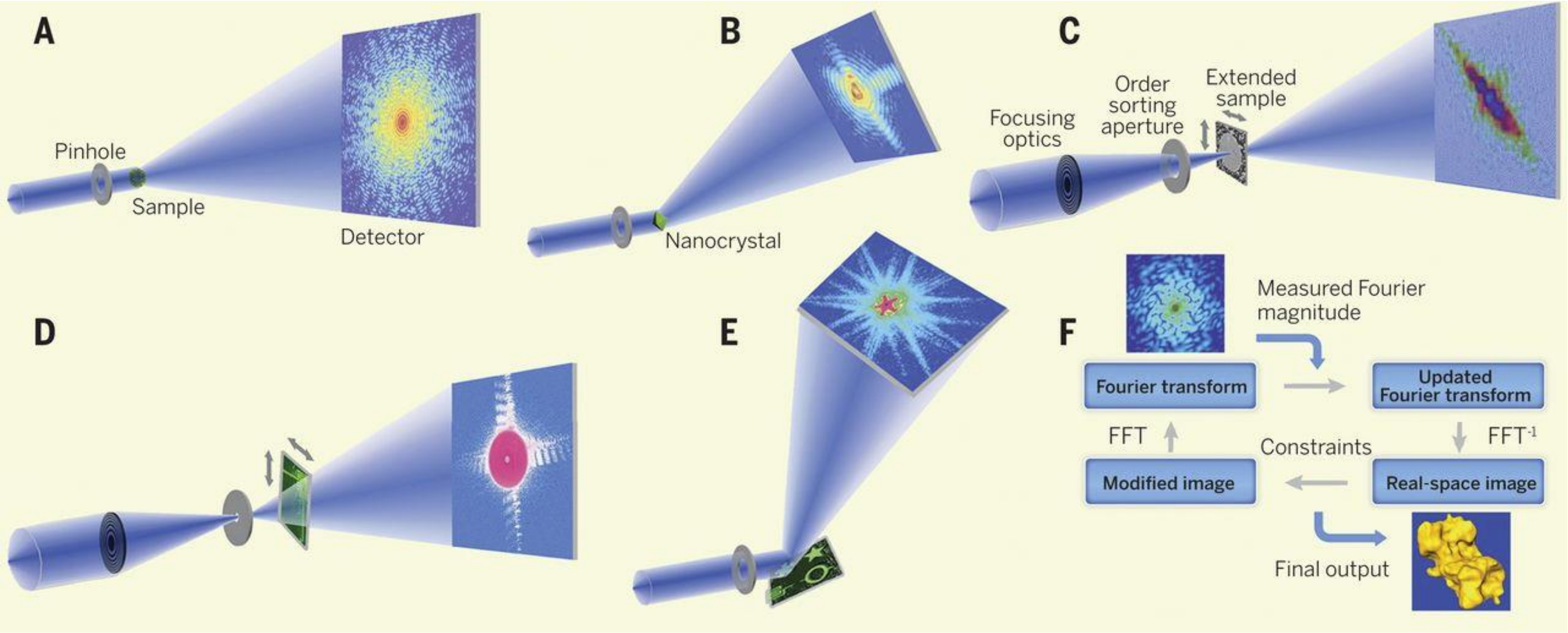

Fig. 1. Schematic layout of five main CDI methods and iterative phase retrieval algorithms. (**A**) Plane-wave CDI: A plane wave illuminates a sample, and an oversampled diffraction pattern is measured by a detector. (**B**) Bragg CDI: The diffraction pattern surrounding a Bragg peak is acquired from a nanocrystal. (**C**) Ptychographic CDI: A coherent x-ray probe is generated by an aperture or focusing optics. An extended sample is scanned through the probe on a 2D grid, and diffraction patterns are collected from a series of partially overlapping regions. (**D**) Fresnel CDI: A sample is positioned in front of (or behind) the focal spot of a coherent x-ray wave, and the Fresnel diffraction pattern is measured by a detector. (**E**) Reflection CDI: A coherent x-ray wave is specularly reflected off a sample on a substrate, and the diffraction intensity around the reflected beam is collected by a detector. (**F**) Phase retrieval algorithms iterate back and forth between real and reciprocal space. In each iteration, various constraints, including support, positivity (i.e., electron density cannot be negative), or partially overlapping regions, are enforced in real space, while the measured Fourier magnitude is updated in reciprocal space. Usually, after hundreds to thousands of iterations, the correct phase information can be recovered.

INS: Principle of *in situ* measurements during growth

GIXS/GIXD/SXRD - Structure

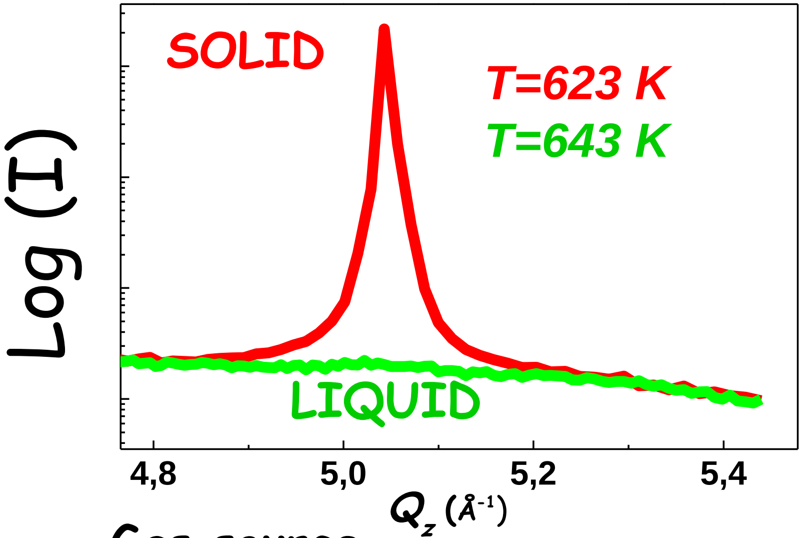

T. Schülli, R. Daudin, G. Renaud, A. Vaysset, O. Geaymond, A. Pasturel, **Nature 464, 1173 (2010)**

GISAXS - Shape

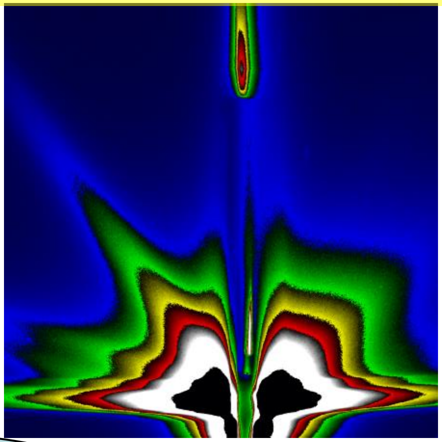

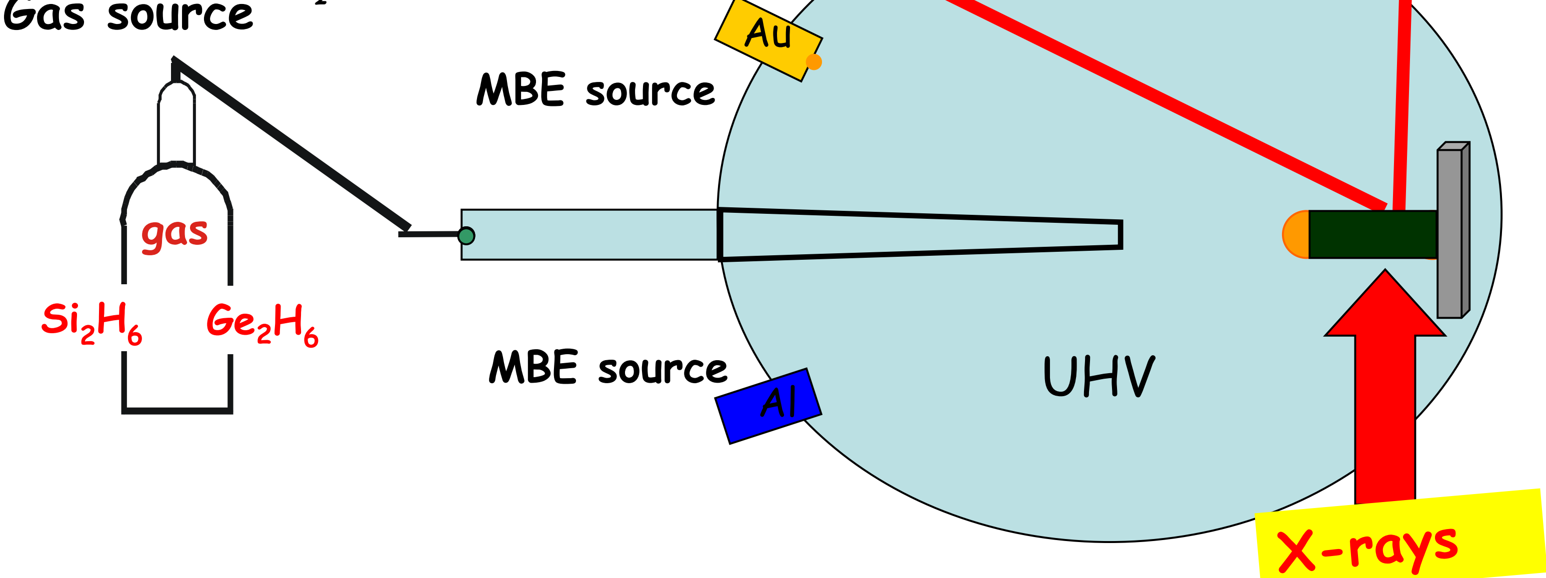

G. Renaud et al.**, Surf. Sci. Rep., 2009**

"Real-Time Monitoring of Growing Nanoparticles",
G. Renaud, et al.**, Science 300, 1416 (2003).**

CRG-IF BM32

In situ UHV-CVD growth of Si/Ge Nanowires

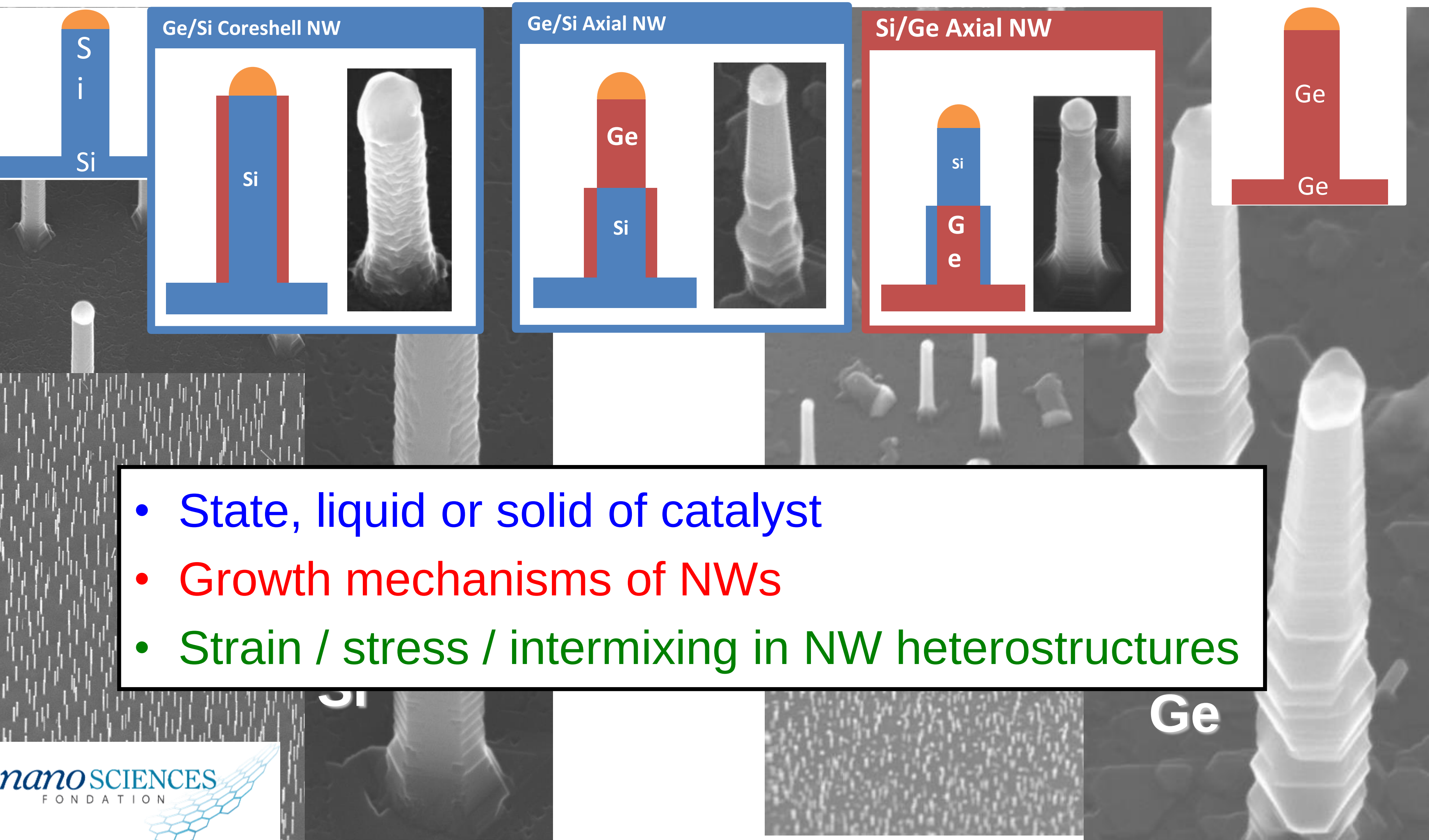

- State, liquid or solid of catalyst
- Growth mechanisms of NWs
- Strain / stress / intermixing in NW heterostructures

Nanobeams to ~~image~~ "count" (1) *GaAs NWs statistical distribution*

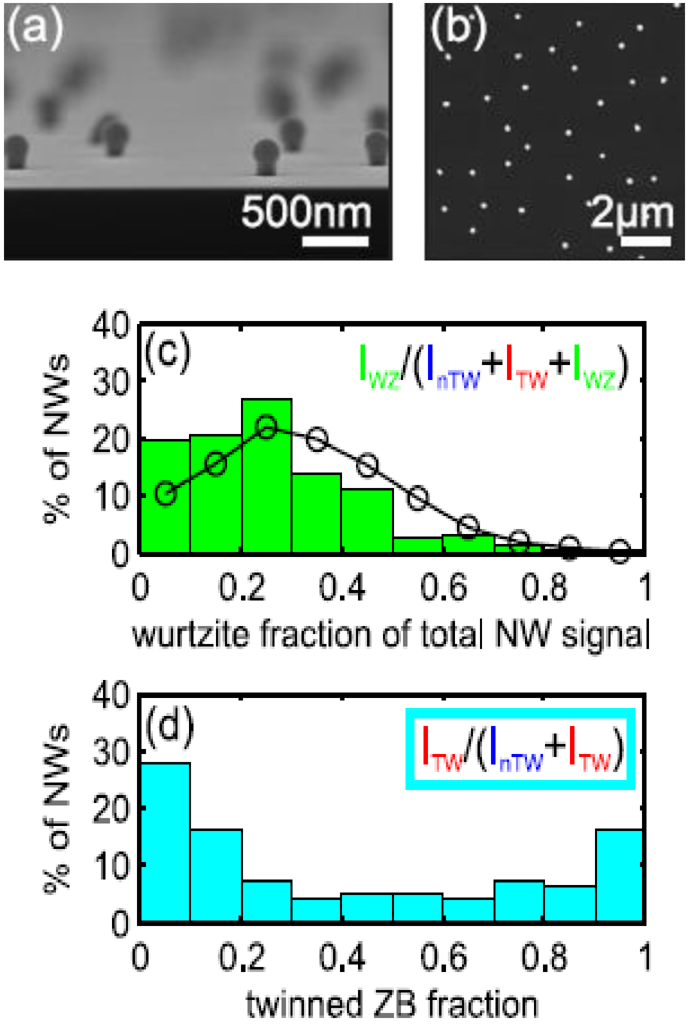

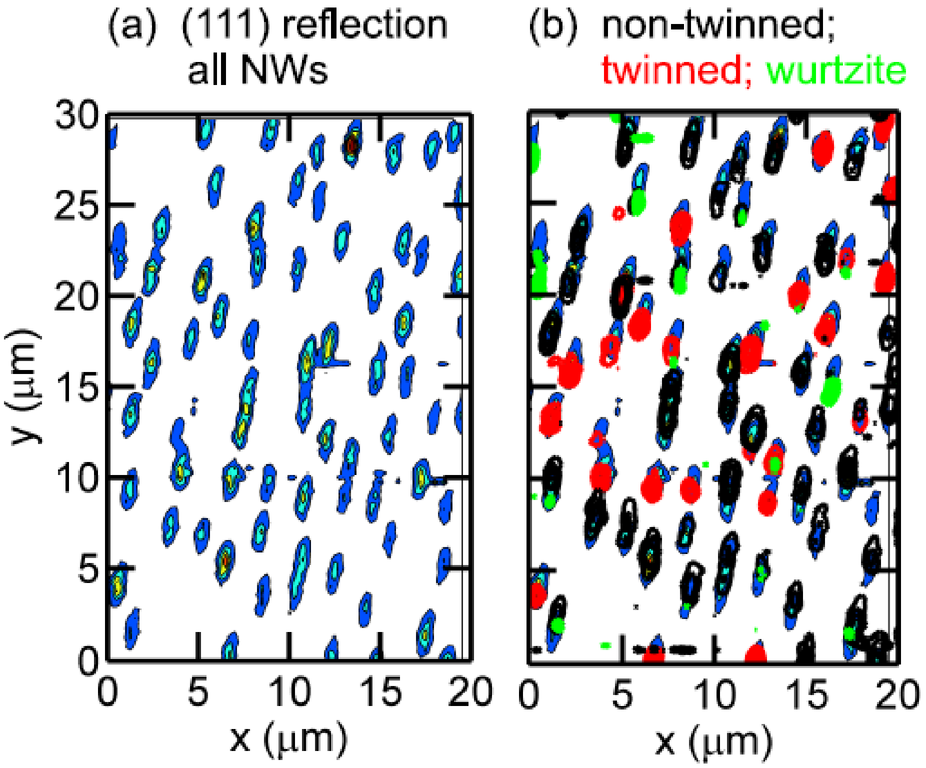

A. Biermanns *et al.*
Phys Status Solidi 2013